



POLITECNICO
MILANO 1863

SCUOLA DI INGEGNERIA INDUSTRIALE
E DELL'INFORMAZIONE

Simplified Fluid Models for the Dynamic Simulation of the Allam Cycle

TESI DI LAUREA MAGISTRALE IN
AUTOMATION AND CONTROL ENGINEERING - INGEGNERIA
DELL'AUTOMAZIONE

Author: **Stefano Riva**

Student ID: 962654

Advisor: Prof. Francesco Casella

Co-advisors: Marcelo Andre Muro Alvarado

Academic Year: 2021-22

Quest'era senza dubbio una rappresentazione efficace dell'ingegneria. Essa costituiva la cornice di un affascinante autoritratto di un uomo dai lineamenti energici, con una pipa fra i denti, un berretto sportivo in testa e splendidi stivali alla scudiera, in viaggio tra Città del Capo e il Canada per realizzare grandiosi progetti della sua azienda. Fra un affare e l'altro si può anche trovare il tempo di ricavare dal pensiero tecnico qualche idea per organizzare e governare il mondo, o di formulare qualche massima. [...] Si rivelarono uomini strettamente legati alle loro tavolette da disegno, amanti della loro professione e in essa ammirevolmente valenti; ma proporre loro di applicare l'audacia dei loro pensieri a se stessi invece che alle loro macchine, sarebbe stato come pretendere che facessero di un martello l'uso contro natura che ne fa un assassino.

L'uomo senza qualità, R. Musil

Abstract

One of the big problems of our era is the growing CO₂ concentration in the atmosphere. Many possible solutions have been proposed and in this study we focus on the Allam cycle, a thermodynamic cycle able to produce electrical power by an oxi-combustion process with high efficiency with zero stack CO₂ emissions.

This cycle has already been studied by the Politecnico di Milano, that, in order to create the most accurate model possible from both a static and dynamic point of view, obtained a very complex model with a huge number of equations. In this thesis here presented, reduced fluid models for the Allam cycle are developed in order to decrease the overall complexity and make the model more manageable. After the development of these reduced fluids, each component and the overall closed cycle were tested both at static and dynamic conditions, comparing the obtained results with the ones obtained with the real fluid. This task was necessary in order to verify that no fundamental information had been lost during the simplification process. After this model validation step, the reduced plant was tested under realistic conditions, with fast load ramps (decreasing from the 100% of the thermal load to 30% in 12.5 minutes). This last analysis had the objective to confirm the flexibility and the performances of the model based control applied to the reduced model.

In conclusion, this study led to good results from both a static and dynamic point of view, simplifying the model without losing too much accuracy.

Keywords: Allam Cycle, CO₂, Model Complexity, Dynamic Modelling, Reduced Fluid Models, Power Plant Control

Abstract in lingua italiana

Uno dei grandi problemi della nostra epoca è il continuo incremento di CO₂ nell'atmosfera. Negli anni sono state proposte molte possibili soluzioni e in questo lavoro ci siamo concentrati sul ciclo Allam, un ciclo termodinamico in grado di produrre energia elettrica mediante un processo di ossicombustione ad alta efficienza con emissioni inquinanti durante il processo praticamente nulle.

Questo ciclo è già stato studiato dal Politecnico di Milano, che, per creare un modello il più accurato possibile sia dal punto di vista statico che dinamico, non ha potuto tralasciare nessun dettaglio, ottenendo un modello molto complesso, con un numero enorme di equazioni. In questa tesi, vengono sviluppati modelli di fluido ridotti per il ciclo Allam al fine di diminuire la complessità generale e rendere il modello completo più gestibile. Dopo lo sviluppo di questi fluidi ridotti, ogni componente e il ciclo chiuso complessivo sono stati testati sia in condizioni statiche che dinamiche, confrontando i risultati con quelli ottenuti con il fluido reale. Questo passaggio è stato necessario per verificare che nessuna informazione fondamentale fosse andata perduta durante il processo di semplificazione. Dopo la fase di validazione del modello, l'impianto ridotto è stato testato in condizioni realistiche, con rapide rampe di carico (decrecita dal 100% del carico termico al 30% in 12,5 minuti). Quest'ultima analisi ha avuto l'obiettivo di confermare la flessibilità e le prestazioni dello schema di controllo applicato al modello ridotto.

In conclusione, questo studio ha portato a buoni risultati sia dal punto di vista statico che dinamico, semplificando il modello senza perdere troppa accuratezza.

Parole chiave: Ciclo Allam, CO₂, Complessità del Modello, Modellazione Dinamica, Modelli di Fluido Ridotti, Controllo d'Impianto

Contents

Abstract	iii
Abstract in lingua italiana	v
Contents	vii
1 Introduction	1
1.1 Objectives	3
1.2 Thesis Overview	4
2 Supercritical CO₂ Cycles	5
2.1 Supercritical CO ₂	5
2.1.1 Thermodynamic Properties	6
2.2 Thermodynamic Cycles	7
2.2.1 Transcritical and Supercritical Thermodynamic Cycles	8
3 Allam Cycle: State of the Art	13
3.1 Allam Cycle	13
3.2 Cycle description	14
3.3 Components	16
3.4 Allam Cycle Advantages	19
4 Model Computational Weight	21
4.1 Complexity Vs. Accuracy	22
5 Modeling Language	23
5.1 Modelica Language	23
5.2 Dymola	24
6 Model Reduction	27

6.1	Fluid Models	28
6.1.1	Real Mixture	28
6.1.2	Pure CO ₂	28
6.1.3	CO ₂ + Water	29
6.1.4	CO ₂ + Oxygen	30
6.1.5	Oxygen Tracking Model	31
6.1.6	Comparison	32
6.2	Compression System	35
6.3	Pumping System	37
6.4	Combustor	39
6.5	Turbine	41
6.6	Regenerator	42
6.6.1	Heat Exchanger	43
6.6.2	Regenerator Model	44
6.7	Allam Cycle Reduced Model	47
7	Open-Loop Responses	51
7.1	Dynamic Behavior	53
7.2	Conclusions	55
8	Model Based Control Logic	63
8.1	Control Structure	63
8.1.1	Low-level Control	63
8.1.2	High-level Control	65
8.2	Results	69
8.2.1	Static Analysis	70
8.2.2	Dynamic Analysis	72
9	Conclusions and Future Developments	81
	Bibliography	83
A	Appendix A	85
B	Appendix B	87
B.1	Peng-Robinson equation of state	87

B.2 Peng-Robinson equation of state for mixtures	88
B.3 Specific heat capacity at constant pressure (c_p)	89
B.4 Enthalpy, Entropy and Internal Energy	89
List of Figures	91
List of Tables	93
List of Acronyms	95
Acknowledgements	97
Ringraziamenti	99

1 | Introduction

In recent years the consequences of global warming have been widely discussed. Climate change has a significant impact on different ecosystems and creates dangerous phenomena such as the increase of the sea level, the increase of temperature in the land and ocean surfaces and the reduction of the arctic ice extent. The underlying cause of it all is the level of CO₂ in the atmosphere that has been continuously increasing in the last centuries. In the last decades, the governments are more and more concerned about this situation and have taken many measures to counter this trend. In particular, since one of the main sources of CO₂ is the burning of carbon-based fuel in energy systems, they strongly encouraged the development of new technologies that could improve the current situation. The graph in 1.1 refers to the behavior of the energy production by energy source in the last three decades. In the last thirty years a lot of work and improvements have been done: the energy production based on carbon-based fuels is constantly decreasing while the production based on renewable energies (solar, wind, hydro) and bio fuels is constantly increasing. Even considering this positive trend, the energy production still largely depends on fossil fuels.

Primary energy production by fuel, EU, in selected years, 1990-2020
Petajoule (PJ)

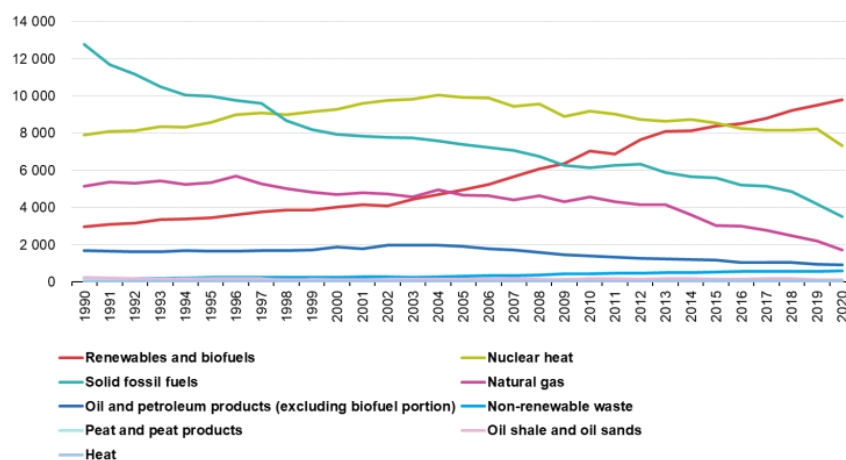


Figure 1.1: European energy production sources behavior [1990-2020][2]

In Italy the conditions are more or less the same (Fig. 1.2), the energy produced by renewable energies is around the 40%, the other 60% is still produced by fossil fuels or imported (10.7%).

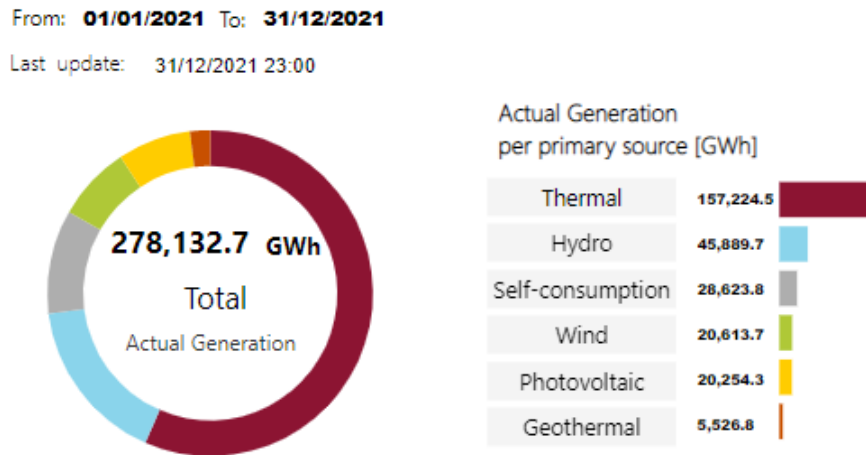


Figure 1.2: Italian energy production sources in 2021[4]

For this reason, in addition to increasing the production of energy with renewable sources, it is also necessary to develop new techniques to reduce the polluting emissions of the fossil fuels power plants. It is in this scenario that the Carbon Capture and Storage (CCS) technologies are being developed. CCS is a combination of technologies that capture and store carbon dioxide deep underground, preventing its release into the atmosphere. It is generally used to help decarbonise industrial processes, such as the production of steel, cement, or chemicals, or to help decarbonise power stations that use hydrocarbons to generate electricity. Anyway, this type of technology presents some huge drawbacks. On one hand, running a carbon capture system is incredibly energy intensive and on the other, there are significant risks related to the disposal and storage of carbon dioxide, a failure during injection (or a blowout) could result in a release of large amounts of CO₂ in the atmosphere.

For all these reasons it could be useful to directly develop power plants able to reduce or totally eliminate the emissions. The Allam cycle could be a way to solve the problem. This cycle works by combusting natural gas with pure oxygen in a combustor, producing CO₂ and water. This fluid is used to spin a turboexpander, producing power. When the flue gas coming from the turbine is cooled down, water is removed and what remains is almost pure CO₂. Thanks to this technology it is therefore possible to obtain a thermodynamic cycle capable of separating the produced CO₂ with a net efficiency around the 50%.

Another aspect to highlight is the flexibility of the system, which would make it very useful if it were necessary to operate it at different loads in short periods.

Even if the Allam cycle is a novel plant, some work has already been done, in particular the energy department of Politecnico di Milano developed a thermodynamic analysis and numerical optimization, obtaining good results in static conditions. Later, the model developed by Muro Alvarado [19], took into account the dynamical behavior of the system.

1.1. Objectives

As introduced in the previous part, the study developed by Muro Alvarado [19] already contains a complete model of the plant, able to well represent static and dynamic behaviors of the system. This model contains a huge number of equations and it is difficult to be manipulated and simulated using state of the art software tools.

The objective of the present thesis is to reduce the model complexity, obviously losing some precision on the static results but obtaining dynamic responses that are not too different, so as to be able to study control systems in a more simple way. A lower model complexity is better from a control point of view because it permits a better and easier implementation of advanced and optimal control techniques and a faster development cycle. The main idea is that it is possible to create new and less complex fluid models that can replace the actual working fluid model, which is a mixture of CO₂ with other gases, in order to decrease the overall complexity of the system.

After this first step, the objective of my thesis is to verify how this fluid model simplifications affect the static and dynamic simulations of the plant. For this reason the static behavior of each component and then of the entire cycle will be tested. The dynamical behavior will be analyzed applying steps to the input variables of the system and looking at the behavior of the output variables. The last thing to do in order to verify the reliability of the reduced fluids is to test the behavior of the plant when the control system is applied. To validate the reduced model, in each one of these steps the obtained results will be compared to the ones obtained using the full model of the working fluid.

From the static point of view, the results obtained with the reduced fluids are practically the same of the ones obtained with the complete fluid. On the other hand, the dynamical simulations in the reduced case present some differences with respect to the complete mixture but the overall behavior is still acceptable for our purposes. Finally, the behavior of the entire reduced model and of the control system under a realistic scenario are pretty good and they confirm the robustness of the applied control scheme.

1.2. Thesis Overview

The dissertation content is structured in the following way:

Chapter 1 It introduces the topic and defines the objectives of the research work. This chapter presents the context and motivation behind the present study.

Chapter 2 In this chapter are illustrated the main properties of the supercritical CO₂ and the main information about the supercritical thermodynamic cycles.

Chapter 3 The relevant information about the Allam cycle are here contained: the developments, a detailed description and its advantages.

Chapter 4 This chapter includes some information about the complexity of a model and how this is related to the work of this thesis.

Chapter 5 This chapter is an overview of the Modelica language with a particular remark on Dymola, the main software used to develop my work.

Chapter 6 In this chapter all the simplifications applied to the cycle are included. It is the core chapter of the study and describes the reduced fluids and the differences when are applied to the components.

Chapter 7 Here an analysis of the step responses of the reduce plant model is performed. It is important to understand which could be the coupling between manipulated and controlled variables.

Chapter 8 In this chapter all the control techniques applied to the scheme are described and then the results in the case of the reduced model are discussed.

Chapter 9 In this last chapter there are the conclusions and possible future developments.

2 | Supercritical CO₂ Cycles

In this chapter the main concepts, knowledge and tools used to develop my thesis are described. The chapter can be considered as a starting point, from which it is possible to expand and mix the ideas in order to achieve new results. In particular in the first section there is a description of the peculiarities of the supercritical CO₂, its uses and its qualities that have brought to its use in power production thermodynamic cycles. In the second one there is a description of the ideas from which the Allam cycle started, the supercritical CO₂ plants. Are also reported the reasons and the peculiarities that led it to be widely used in various fields.

2.1. Supercritical CO₂

Carbon dioxide is a triatomic molecule consisting of a carbon atom in the center, to which two oxygen atoms are bonded through one double bond each. This structure makes it a linear molecule and therefore apolar, which is why it is not flammable and relatively inert at room temperature. At ambient temperature and pressure it is gaseous, colorless and odorless, with a density 60% greater than air (1,225 kg/m³).

Following the studies carried out, the number of possible applications for this fluid is grown considerably, especially in recent years. This is thanks to some important and peculiar characteristics [16]:

- Good stability at high temperatures
- Critical conditions achievable at low temperatures and pressures
- High availability in nature and low cost

The supercritical condition is a fluid state in which its temperature and pressure are held at (or above) its critical temperature and critical pressure (Fig. 2.1). Carbon dioxide behaves as a supercritical fluid above its critical temperature (304.25 K or 31.1 °C) and critical pressure (73.9 bar or 7.39 MPa), expanding to fill its container like a gas but with a density like that of a liquid. When fluids and gases are heated above their critical temperature and compressed above their critical pressure they enter a supercritical phase

where some properties can be dramatically changed [9].

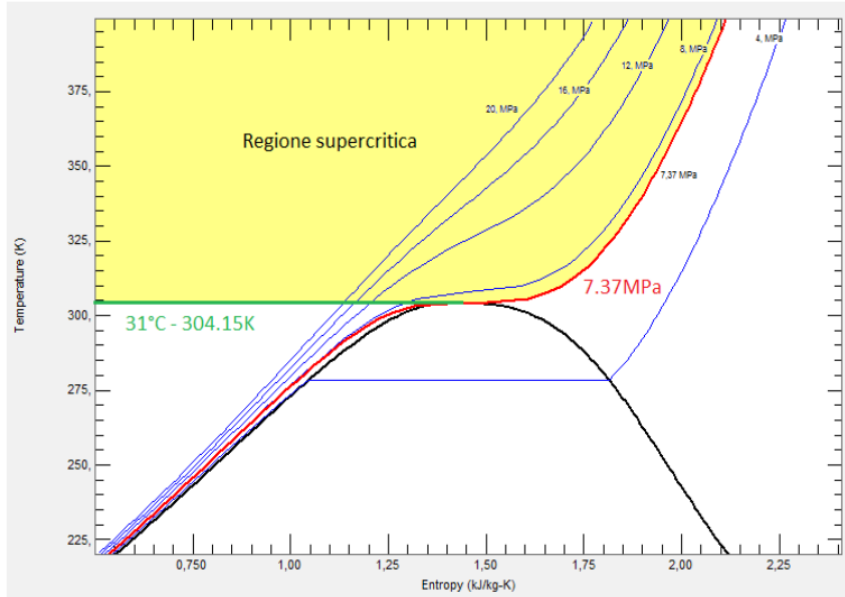


Figure 2.1: CO₂ phase diagram [20]

2.1.1. Thermodynamic Properties

As shown in Fig. 2.2,2.3,2.4 and 2.5, the thermophysical properties of CO₂ change dramatically with temperature and pressure in the supercritical region. For a given pressure, thermal conductivity, dynamic viscosity and density are strongly decreasing with the increase of temperature. Moreover, the isobaric heat capacity presents a peak at critical point and pseudocritical temperatures, which is reduced as the pressure increases. These heat capacity sharp peaks are similar to the ones obtained in phase change processes of mixtures used for thermal energy storage purposes, however, the dramatic decrease of density limits the potential of the S-CO₂ to be used as storage media. These variations of the fluid make its heat transfer performance different from conventional fluids, especially in the determination of the convective heat transfer coefficient from a heat transfer surface, and the steady state supercritical natural circulation flows [9].

This particular behavior introduces some troubles both in the cycle design and in numeric simulations. In particular they are relevant in the heat exchangers design. The thermo-physical properties that controls the heat transfer capabilities of a refrigerant are: density, specific heat capacity at constant pressure, thermal conductivity and the dynamic viscosity. The last three properties permits the estimation of the Prandtl (2.1) number, a dimensionless parameter, which is used in the correlations for the calculation of the heat

transfer coefficients.

$$P_r = \frac{C_p \mu}{k} \quad (2.1)$$

From this brief analysis, it clearly appears that it is not possible to consider the thermo-physical properties nearby the critical point constant. The sudden variations and the peaks can lead to unmanageable error during the heat exchangers design [7].

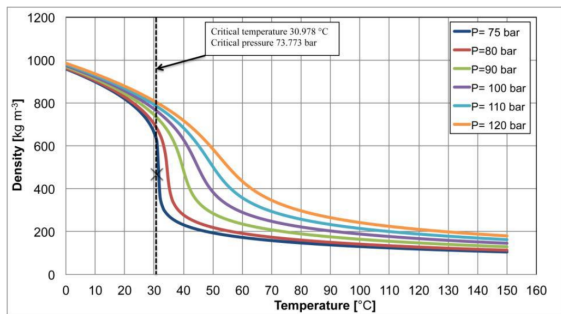


Figure 2.2: Density ρ

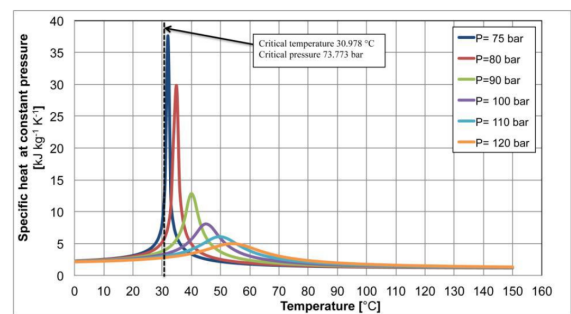


Figure 2.3: Specific heat C_p

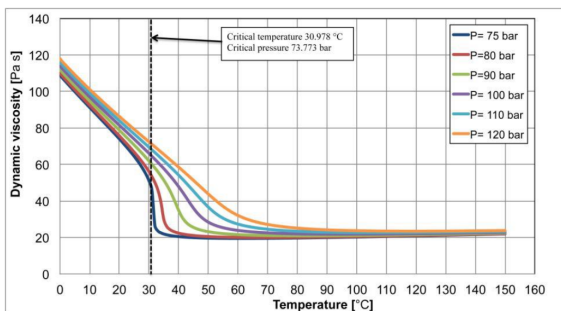


Figure 2.4: Dynamic viscosity μ

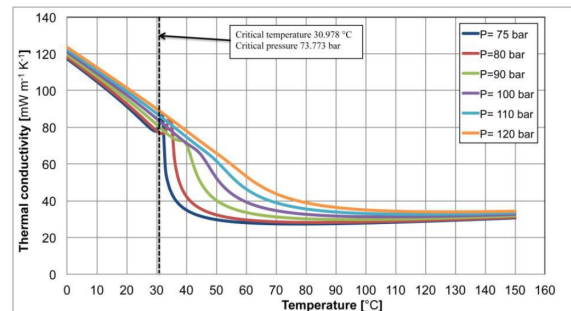


Figure 2.5: Thermal conductivity k

2.2. Thermodynamic Cycles

Typical thermodynamic cycle consists of a series of thermodynamic processes transferring heat and work while varying pressure, temperature, and other state variables, eventually returning a system to its initial state. The classic power generation cycles are divided into two different families: gas cycles and vapor cycles. In gas cycles the working fluid remains in the gas phase throughout the cycle, while in the vapor ones usually a boiler or evaporator as well as a condenser are included so that the working fluid is a gas at some points in the cycle and a liquid at others. Thermodynamic cycles can be categorized in yet another way, as closed and open cycles. In closed cycles, the working fluid is returning

to the initial state at the end of the cycle and is recirculated. In open cycles, the working fluid is renewed at the end of each cycle instead of being recirculated. For example, in automobile engines, the combustion gases are exhausted and replaced by fresh air–fuel mixture at the end of each cycle, differently in a closed Brayton cycle the flue gas of the turbine is captured and compressed again to restart the cycle [27].

2.2.1. Transcritical and Supercritical Thermodynamic Cycles

At this point, in order to understand why supercritical and transcritical CO₂ cycles are being studied so much over the years and being the Allam cycle an application of these technologies, it is important to introduce some concepts about them. A cycle is defined as "supercritical" when all the thermodynamic transformations occur under conditions of temperature and pressure above the critical point. If instead the transformations occur both above and below the critical point, then the cycle is called “transcritical” (Fig. 2.6) [18].

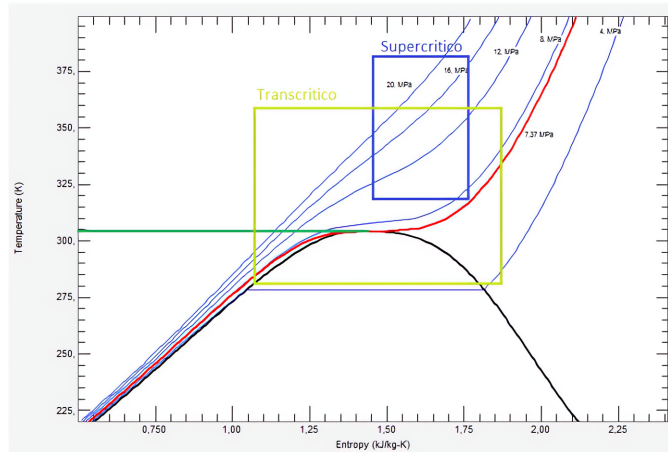


Figure 2.6: Work zones for supercritical and transcritical cycles

Supercritical power cycles operates as already stated, near the critical point to take advantages from the variations in thermodynamic property and increase their efficiency [7]. The theoretical maximum efficiency that can be reached by a a thermodynamic cycle is fixed by the *Carnot's rule* (2.2), where T_c and T_h are respectively the cold and hot temperature of the cycle. It is straightforward to understand that, given the cold temperature, the higher is the hot temperature, the higher is the efficiency of the cycle. Real cycles are irreversible and thus have inherently lower efficiency than the Carnot efficiency when operated between the same temperatures T_c and T_h .

$$\eta_{Carnot} = 1 - \frac{T_c}{T_h} \quad (2.2)$$

In the field of energy production there exist different types of power plants feed by several heat sources. By comparing the thermal efficiencies of several conversion systems with respect to the Turbine Inlet Temperature (TIT) range, it is possible to make a comparison of them. In figure 2.7 can be observed the efficiency of different power plants, in particular they are the organic Rankine cycle (ORC), steam Rankine cycle (steam turbine), air Brayton cycle (gas turbine), combined cycle gas turbine (CCGT), and S - CO₂ direct and indirect cycles.

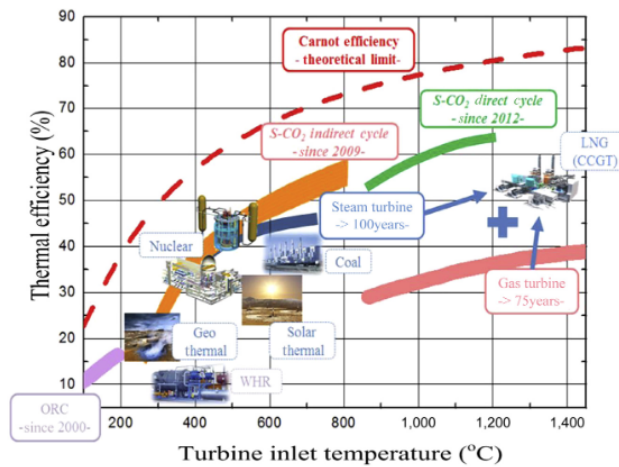


Figure 2.7: Thermal efficiencies of power conversion systems with respect to the TIT

As shown in the figure above, the steam Rankine cycle can achieve high efficiency under low turbine inlet temperature conditions because the working fluid is compressed at a liquid state. In other words, liquid water has high density and requires less work for compression. In contrast, the gas turbine utilizes air, a compressible fluid, and a large amount of work is consumed for the compression process. Therefore, the thermal efficiency of gas turbines is not significantly higher than that of a steam Rankine cycle although the turbine inlet temperature is much higher because the compressor requires a large amount of work [24].

The best solution to increase the conversion efficiency is the closed S - CO₂ Brayton cycle. Adopting this solution the advantages of both steam Rankine cycle and gas turbine system are combined. The fluid is compressed near the critical point where the isobars on the T-h diagram have a low slope and they are very close to each other. This low slope is directly translate to a compression process where energy can be added to the fluid while incurring in a small increase of the fluid temperature (high specific heat C_p). By reducing the amount of energy required to increase S - CO₂ pressure, the amount of work input on the cycle is extremely reduced compared to the work extracted from the cycle and this directly affect the cycle efficiency.

This behavior that directly affects the behavior of turbo-machines can be better understood by analyzing the compressibility factor (Z), that is a correction term which describes the behavior deviation of a real gas from an ideal gas. Is calculated as in 2.3, where p is the pressure, ρ is the density of the gas and $R_s = \frac{R}{M}$ is the gas constant with M the molar mass and T the temperature.

$$Z = \frac{p}{\rho \cdot R_s \cdot T} \quad (2.3)$$

It is simply defined as the ratio of the molar volume of a real gas to the molar volume of an ideal gas at the same temperature and pressure. The value of Z generally increases with pressure and decreases with temperature, for an ideal gas its value is 1 by the definition. The closer the gas is to its critical point or its boiling point, the more Z deviates from the ideal case. Due to these reasons would be better perform the compression in thermodynamic condition with $Z < 1$ in order to reduce the required compression work. On the contrary, it is appropriate to expand the fluid when it is close to the ideal conditions. For the CO₂ near the critical point, the compressibility factor decreases up to 0.2-0.5 as shown in 2.8, and the compression work can be significantly reduced. This phenomenon leads to an increase of the useful work and consequently of the cycle efficiency.

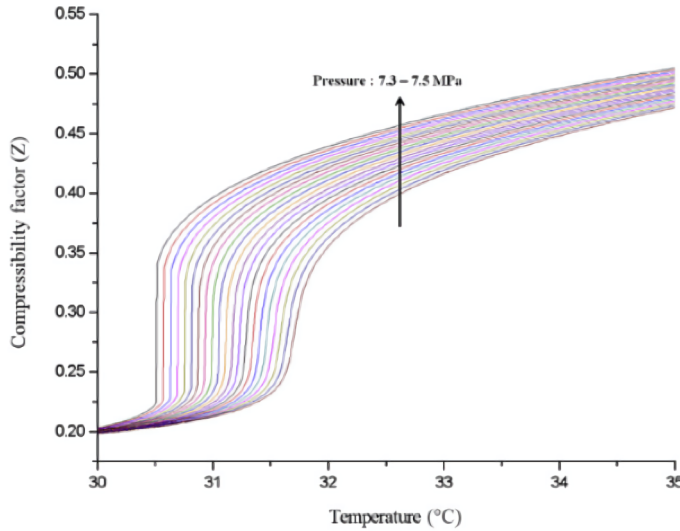


Figure 2.8: CO₂ compressibility factor behavior

Another significant advantage of the high density of the supercritical CO₂ is that it allows to use very compact turbomachines, very different from the normal machines that work with other fluids. This compactness reduces material costs and makes the lighter turbomachinaries suitable for naval or solar applications. On the other hand, machines with similar pressure, temperature and density values are not included in known standards,

such as gas and steam turbines. Develop a good design is therefore a challenge. In our particular case, the model of the turbine that will be discussed in 6.5 is not traditional and it is based on on the previous specific work of Scaccabarozzi et al. [23].

In this last part of the chapter we will analyze the overall efficiency of different power plants. In figure 2.9 can be observed the behaviors of the efficiencies of four thermodynamic cycles: a supercritical CO₂ cycle, a helium Brayton cycle, a supercritical steam cycle and a superheated steam cycle. Comparing the efficiencies between a supercritical CO₂ cycle, a helium cycle and a Rankine cycle it is clear that if the TIT assumes values higher than 550°C the S-CO₂ cycle is better than the Rankine. At lower temperatures, however, the steam cycles (supercritical or superheated) achieve higher cycle efficiencies than S-CO₂ cycles. In conclusion, there are multiple reasons why S-CO₂ cycles deserve

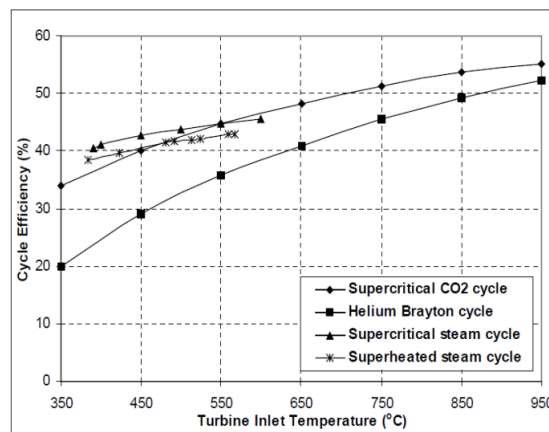


Figure 2.9: Different cycle efficiencies with respect to the TIT [13]

to be investigated. Most important of these are [18]:

- Carbon dioxide is a fluid already used in some industrial fields (e.g. as a solvent) and its thermodynamic properties are well known. It is abundantly present and available, stable, non-toxic, non-corrosive, non-flammable and low cost
- The cycle efficiency is high, and this is mainly due to the low compression work required close to the critical point
- The components are very compact
- The critical point (31°C) allows the use of water at ambient temperature for heat rejection
- The cycle has a high power density

- The cycle operates well at partial loads [23], so it is good to complement intermittent renewable energy sources such as wind and photovoltaic

3 | Allam Cycle: State of the Art

In this chapter the Allam cycle will be described. In the first section is presented the birth and all the subsequent studies and development done on this cycle up to now. Here is also presented the starting point for my thesis, the model created by Muro Alvarado [19]. In the second section is reported a detailed description of the thermodynamic cycle with all the transformations to which the fluid is subjected. The third section is a listing of the components present in the cycle. Every component is described from the physical point of view and from his function in the cycle and its interaction with other components and streams. Finally in the last section are reported the technological benefits that brought this cycle to be so studied and analysed over the years.

3.1. Allam Cycle

The Allam Cycle was invented by Rodney Allam, a chemical engineer who has worked in industry throughout his career. It is a novel CO₂ oxy-fuel power cycle that utilizes hydrocarbon fuels while inherently capturing approximately 100% of atmospheric emissions (except the ones related to the upstream natural gas production process), including nearly all CO₂ emissions at a cost of electricity that is expected to be highly competitive with the best available energy production systems that do not employ CO₂ capture. Traditional power cycles require the addition of expensive, efficiency-reducing equipment in order to reduce and capture emissions of CO₂ and other pollutants. Analyses of these cycles have shown that the additional CO₂ removal systems can increase the cost of electricity by 50% to 70% when capturing typically 90% of the CO₂ generated from hydrocarbon fuel combustion. The Allam Cycle takes a novel approach to reducing emissions by employing oxy-combustion and a high-pressure supercritical CO₂ working fluid in a highly recuperated cycle. The CO₂ that must be vented from the process leaves at pipeline pressure and high quality as a result of the operating conditions of the cycle, thereby mitigating the common necessity of an additional capture, clean-up, and compression system [6].

Allam Cycle was officially patented in USA on Dec. 3, 2013. The same year, Allam

et al. [5], in representation of NET Power, Toshiba Corporation, Exelon Corporation and the Shaw Power Group, presented the first publication of this power cycle, explaining the general description of the process, a high level description of the main components, the efficiency targets of the cycle using natural gas or coal as fuel, and the plan to build a 50MWt natural gas power plant. One of the first relevant studies done in Italy was developed by Politecnico di Milano and Amec Foster Wheeler Italiana. They developed and analysed a full model of the Allam Cycle, technical and money wise. Moreover, they modelled a gas turbine in detail, including parameters requirements such as efficiency, stage number and blade cooling [19].

During the years a lot of studies and development have been done on this cycle. The starting point of my thesis is one of these works, in particular is the work done by Muro Alvarado [19] for his master thesis at Politecnico di Milano. He modeled a full Allam Cycle power plant, analyzing its dynamics and evaluating the complexity of its controllability in on-design and off-design conditions. In particular he developed a model of CO₂ gas mixture, including water-vapour condensation phenomena and a model for each component, especially the one of the regenerator. He tested and validated the entire plant model and analyzed its dynamic behavior, defining whether or not can be controlled at different part loads with a simple PID or an advanced controller is absolutely necessary.

3.2. Cycle description

In this section the cycle and all the transformations that occur in the different phases and zones are described. In figure 3.1 a schematic representation of the cycle and the names given to each stream used for the description below can be observed. The nomenclature is the one used by Scaccabarozzi, Gatti and Martelli [23] in their previous work on this cycle.

The closed process is structured as follows: the Allam cycle uses a high pressure oxy-fuel combustor, in which enter an oxidant stream (stream OX-03), the fuel (CH₄) and a recycled stream of CO₂ (stream RE-05) to moderate the flame temperature. The high-pressure stream produced by the combustor (stream FG-01), after being cooled in the inlet by a fraction of another recycle stream of CO₂ (stream CF-02) to an acceptable temperature, moves to a high-temperature, high-pressure turbine. The turbine works with an inlet pressure around 300 bar, while its pressure ratio is around 10.

The exhaust flow of the turbine (stream FG-02) flows through the regenerator, transferring heat to both streams: the recycle stream sent to the combustor as temperature moderator and the recycle stream sent to the turbine as inlet cooling flow. After being cooled in

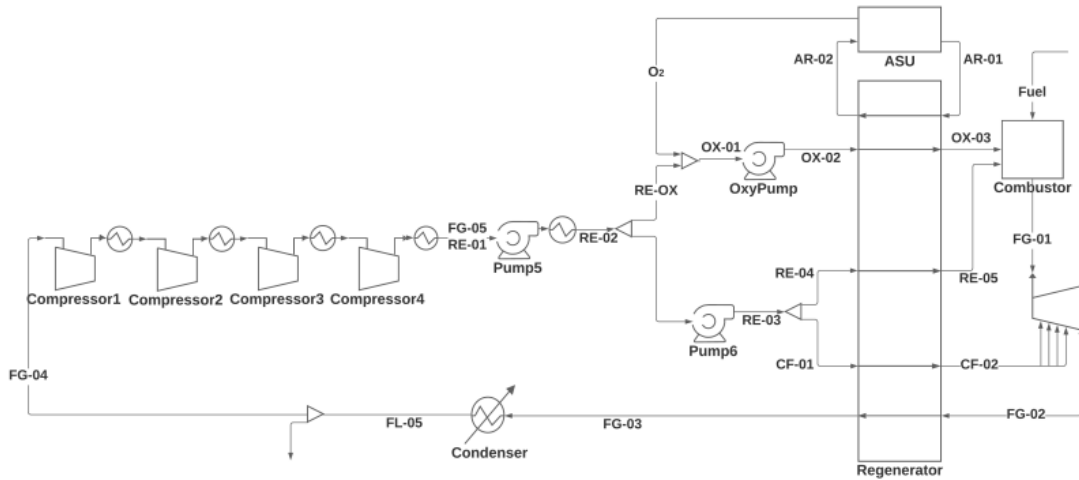


Figure 3.1: Allam cycle process flow diagram

the regenerator (stream FG-03), the exhaust flow of the turbine is cooled again near to atmospheric temperature by a condenser. Here, the vapour coming from the combustion of CH_4 is condensed and then removed, leaving a dominant CO_2 stream (stream FL-05). Some of this CO_2 is sent to the storage (5%) while the rest (stream FG-04) is compressed by the compression system, composed by four compressors in series, which increases the pressure above the critical value (around 80 bar). This supercritical CO_2 stream is then cooled down to atmospheric temperature (stream FG-05) so that a high density can be achieved (around 700 kg/m^3). The pressure of this recycled stream is increased up to the pressure value of the oxygen stream provided by the Air Separation Unit (ASU) (stream RE-02). Then, part of the recycle stream (stream RE-OX) is mixed with the oxygen flow to produce the oxidant stream (stream OX-01) and is pumped to the regenerator (stream OX-02), the other part is pumped to the maximum cycle pressure (stream RE-03) using a centrifugal pump and then it is divided into two streams (streams RE-04 and CF-01). Both streams go through the regenerator and then to the combustor, closing the loop [19].

From 3.2 can be observed the main operating points of the cycle represented on Pressure-Specific Enthalpy diagram.

- **A** \rightarrow **B** From point A (turbine inlet 1150°C , 300 bar), the fluid is expanded by the turbine until point B (30 bar)
- **B** \rightarrow **C** The flue gas passes through the regenerator and the heat is recovered and transmitted to the recycle stream
- **C** \rightarrow **D** Water separation at room temperature takes place

- **D** → **E** The fluid enters in the compression system composed by four compressors interconnected by four intercoolers in order to maintain the temperature around 25°C and reduce the compression work by increasing the inlet density of the subsequent stage
- **E** → **F** , the pressure of the fluid is raised by a multi-stage centrifugal pump up to 300 bar
- **F** → **G** The recycle stream is heated up in the regenerator
- **G** → **A** The heated recycle CO₂ flow enters the combustor, where it mixes with methane stream and oxidant stream

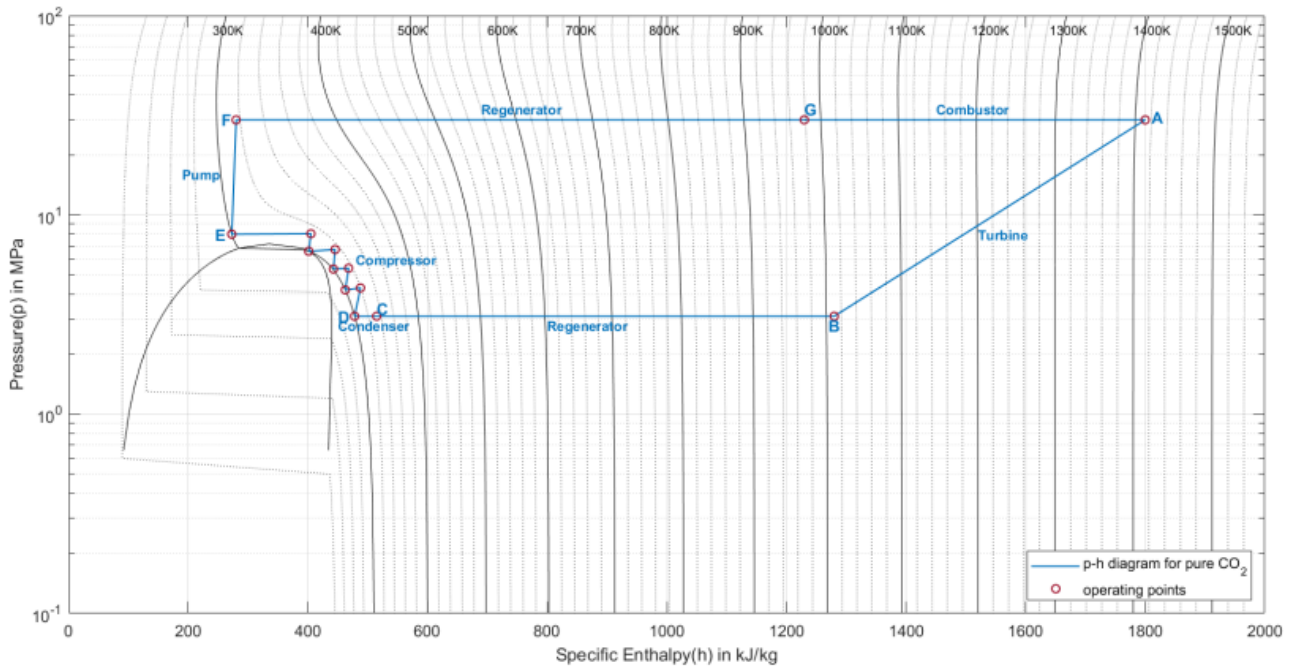


Figure 3.2: Allam cycle Pressure-Specific enthalpy diagram for pure CO₂

3.3. Components

Here below are reported all the components present in the cycle:

- **Fluid**

The fluid used in the cycle is one of the fundamental points of my thesis. The fluid considered in the previous work of [19] is a mixture composed by 5 elements (CO₂, O₂, N₂, H₂O and A_r) and modeled with Peng-Robinson Equations of State (PREOS). The fact that is not a pure substance and the choice of Peng-Robinson

equations to model its behavior results in a huge number of equations in the overall model.

- **Compression System**

The compression system of the plant is composed by four compressors in series interconnected with four intercoolers.

The objective of the compression system is to compress the mixture of CO₂ coming from the condenser from 30 bar to 80 bar, keeping the density as high as possible at the inlet of each compressor, to reduce the compression work which is inversely proportional to the density. This phenomena derive from the thermodynamic properties of S-CO₂ described in 2.1.1. On the other hand, the objective of the intercoolers is to maintain the temperature of the gas at the inlet of each compressor close to the saturation.

- **Pumping System**

The pumping system in the process is composed by three pumps. The first pump, called as "P5" (Fig. 3.1) is in charge of sending the stream of CO₂ to the next two pumps by increasing its pressure from 80 to 120 bar, which is the minimum pressure for the safe flow of oxygen from the ASU. The outlet stream is divided into two, the first one is pumped to pump "P6" and the second one is mixed with a stream of oxygen and then pumped to "Poxy". After "P6", the stream is divided in two parts, going both through the regenerator (moderator stream). The "Poxy" sends the fluid of condensed CO₂ and O₂ to the regenerator (oxidant stream).

- **Combustor**

The combustor present in the cycle has three input flows and one output flows. The input are the fuel, mainly composed by methane, the oxidant stream, composed by CO₂ and O₂ and the recycle stream, composed by pure CO₂ that is needed to regulate the temperature of the flue gas to prevent the damage of the turbine.

The carbon dioxide represents approximately 95% of the mass flow in the combustor while oxygen and methane represents together the other 5%.

In the combustor, a chemical reaction occurs, the flue gas produced due to this reaction goes to the turbine with a working nominal temperature around 1150°C.

- **Turbine**

The turbine receives 2 input fluxes: the outlet flue gas from the combustor with a pressure around 300 bar which is decreased to 30 bar (pressure ratio of approximately 10), creating electrical power and a stream of pure CO₂ (moderator) in order to cool down the blades temperature to avoid damaging the turbine, obtaining at the outlet

of the turbine a temperature around 725°C.

As will be described in more detail in 6.5, the turbine is unconventional and the characteristics that makes it to be special are the following [23] :

- The turbine inlet temperature is slightly lower than a modern gas turbine
- The maximum pressure of the cycle has a value comparable with those of advanced steam turbines
- An unconventional working fluid flows through this equipment

- **Regenerator**

The regenerator is the main component of the Allam Cycle. The objective of the regenerator is to transfer heat from the different streams of the process, obtaining maximum efficiency; in other words, the efficiency of the cycle depends mainly on the performance of the regenerator.

The objective of the regenerator is to recover heat not only from the turbine exhaust but also from the hot air coming from the ASU. The regenerator works in the hot side with temperatures around 700 - 750°C and manages high-pressure differences in the range of 350-250 bar between the hot and cold streams.

There are five streams that go through the regenerator. Three cold streams which are the oxidant stream coming from the pump "Poxy" and the recycle and the cooling stream both coming from pump "P6". The first two streams go from 50°C to 700°C approximately, while the third one goes from 50°C to 150°C approximately. Two hot streams which are the flue gas stream coming from the turbine and the hot air stream coming from the ASU. At nominal conditions, the flue gas goes from around 725°C to 60°C and the hot air goes from 273°C to 60°C.

One important event that occurs in the regenerator is the water condensation in flue gas, contributing with more heat to be exchanged [19].

- **Condenser**

The condenser receives the flue gas at 62°C from the regenerator and decreases its temperature to ambient temperature. Moreover, the condensed water is removed from the gas, letting the gas at the outlet to be almost pure carbon dioxide.

- **Air Separation Unit**

The ASU is used to supply the oxygen needed for the combustion. The oxygen concentration of the output stream of the ASU is around 99.5% thus the oxygen stream is then mixed with supercritical recycled CO₂ in order to obtain the desired oxygen concentration in the range of 15 - 30%. This stream is then compressed by

the pump "Poxy", preheated inside the regenerator and ends up in the combustor.

3.4. Allam Cycle Advantages

In this last section are summarized the technological benefits given by the Allam cycle:

- Net efficiency of the cycle between 45% - 55%
- Higher conversion efficiency with carbon capture
- Ability to work at low load levels without excessive penalty in terms of cycle efficiency
- Important water savings compared with integrated gasification combined cycle technology
- Flexibility to work with different types of fuel

4 | Model Computational Weight

In this chapter the issue of computational weight and complexity in models simulation will be discussed. The complexity of a simulation model is defined as a measure that reflects the requirements imposed by models on computational resources. These requirements can be characterized in various different forms:

- The memory space the program requires in the computer to represent the model structure
- The time it takes to simulate one realization of the model
- The time and effort involved in constructing, implementing, testing, modifying, maintaining, and communicating the model.

Ultimately, the complexity of a model can be measured in terms of the extent of the resources it needs for development and simulation; this complexity is often related to the structural properties of the model [15].

As already said in the introduction (1), one important objective of my thesis is to simplify the models in order to decrease the total complexity of the plant model. There exist a lot of approaches used to simplify a model, in this case, the attempt is to simplify the fluid model used in the cycle. This choice is given by the fact that the model of the fluid already present in the model is composed by five chemical species and PREOS (appendix B) are used to model its behavior. These choices directly reflects on the huge number of equations that need to be solved to simulate and control the system.

Our simplifications aim to reduce the complexity of the fluid, decreasing the number of equations, the computational load and finally the simulation times. This procedure is applied in order to obtain faster simulations and simpler models, things that from a control point of view can improve the design of control logics and could also simplify the application of advanced optimal control techniques.

4.1. Complexity Vs. Accuracy

A point that need to be discussed now is the one about the relationship between complexity and accuracy. It would appear obvious that when presented with two simulation models of the same system, the one which incorporates more aspects of the real system will be the more accurate. In other words, higher fidelity, and by nature more complex, models are more accurate. A valid model is one that is sufficiently accurate for its purpose and so as long as a simplification does not force a model below the desired threshold of accuracy, the validity criterion is still achieved [22]. The aim of the thesis is to determine how much we can decreased the complexity without falling below the accuracy threshold. Or in other words, we will study the impact of several types of model simplifications on the trade-off between model accuracy and complexity for the entire Allam cycle model. This relationship will be investigated by applying different levels of simplification to the simulation model and measuring the impact on the final behavior of the plant.

In Chapter 6 the simplifications applied to the fluid will be described in detail, starting from the simplest model composed by pure CO₂ to the model composed by two chemical species. In the same chapter there is also a comparison between these models applied to the same scenario, highlighting which can be used without falling below the accuracy threshold and which can not, eventually reaching a good trade-off between the complexity and the accuracy of the model.

5 | Modeling Language

In this chapter is described the language and the software used to develop all the models, the tests and the control schemes presented subsequently in the thesis. In particular in the first section there is a description of Modelica, the modeling language, in the second one an overview of the Modelica existing library specific for power plants and finally, in the last section there is a description of the simulation environment used for the development, Dymola.

5.1. Modelica Language

Modelica is an object-oriented, declarative, multi-domain modeling language for component-oriented modeling of complex systems. The Modelica language is developed by the non-profit Modelica Association [3] that also develops the open Modelica Standard Library that contains thousands of generic model components and functions in various domains. Modelica is convenient for a series of reasons. Using complex algorithms in background, Modelica compiler allows engineers to focus on high-level mathematical description of component behaviour and get high performance simulation capability without having a deep knowledge about complex topics such as differential-algebraic equations, symbolic manipulation, numeric solvers, code generation, post-processing (5.2) and without wasting time to deal with all these issues. The fundamentals features of the language are the following:

- *A-causality*: the equations are written in a declarative form, independently from the boundary conditions and without defining model inputs and outputs as in the casual approach, which allows to represent the components in the more natural and physically coherent manner
- *Encapsulation*: the models obtained through the a-causal approach interact with each other using interfaces (connectors), a fundamental point that permits the reuse of models or their substitution in an easier way
- *Inheritance*: is the possibility of creating general models valid for a large class of

components and then specialize them each time by adding new equations, variables or other models as well

- *Multi-domain Modeling*: components of different domains can be combined together in the same system
- *Re-usability*: the reusability of the models is a consequence of the properties of a-causality, encapsulation and inheritance. The standard library is the starting point for each project and has, in addition to many already final components, other generics that can be specialized.

Modeling of Power Plants

To analyse the Allam Cycle, that is the energy power plant under our study, it is very useful the use a modeling language such as Modelica. This system in fact is characterized by different physical phenomena and components belonging to several domain, and hence, the employment of this particular language facilitates its comprehension and the possibility to further improvement on it.

Concerning with the modelling of power plants using Modelica language, there are various research that have been developed during the last years. The first ThermoPower Library [11] was presented by F. Casella and A. Leva [12], this open-source library has been developed to study the dynamic modelling of thermal power plants and energy conversion systems. After this, other libraries have been developed over the years.

Regarding the Allam Power Cycle, there is no bibliography that focus on the modelling and simulation of this cycle using an object-oriented approach like Modelica does. The work of Muro Alvarado [19] can be considered as the first step in this direction. Its work is also used as reference library for my thesis work.

5.2. Dymola

In this last section the simulation environment used to create the models of the thesis is described . In general, a simulation environment is a software able to interpret the language, in our case Modelica language, possibly checking for errors, and then translate it into machine code, converging to a solution as efficiently as possible.

There exists a lot of different environments that allow to work with Modelica modeling language, however, for all these softwares, it is possible to read the same code due to the standard attribute of Modelica. The Modelica association makes the Modelica Standard Library available to everyone, making possible to reuse predefined components and libraries.

For the present work the software that has been used is Dymola. Dymola is a commercial modeling and simulation environment based on the open Modelica modeling language. Dymola was initially designed in 1978 by Hilding Elmqvist, for his PhD thesis at Lund Institute of Technology (later part of Lund University). In 1992, Elmqvist created the Swedish company Dynasim AB to continue the development of Dymola and in 2006, Dassault Systèmes acquired Dynasim AB and started to integrate Dymola in CATIA.

Dymola has multi-engineering capabilities which mean that models can consist of components from many engineering domains. Using the Modelica language, sub-systems are represented by interconnected components; at the lowest level dynamic behavior is described by mathematical equations or algorithms. Dymola processes the complete system of equations in order to generate efficient simulation code. Domain-specific knowledge is represented by Modelica libraries, containing components for mechanical, electrical, control, thermal, pneumatic, hydraulic, power train, thermodynamics, vehicle dynamics, air conditioning, etc [1].

Object-oriented models of complex physical systems can have a very large number of equations and variables. In figure 5.1 can be observed the transition passages from the Modelica code to the simulation one.

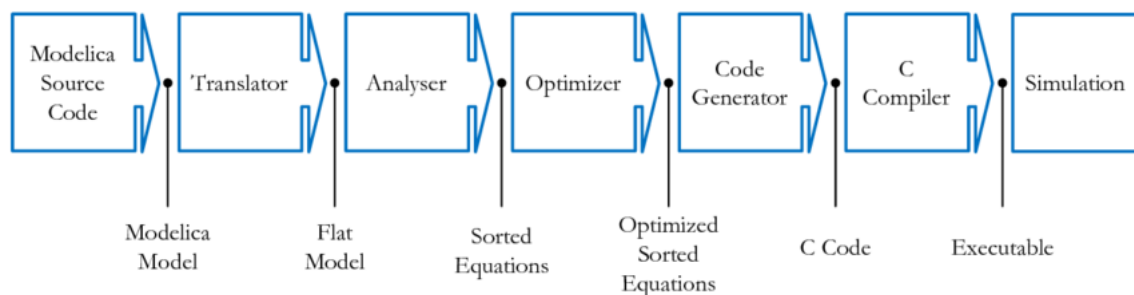


Figure 5.1: Translation stages from Modelica code to executing simulation

Here below will be briefly described the steps [17]:

- **Translation**

The Modelica source code (*.mo* file) given as input to the compiler is first translated to the so-called "*flat*" representation of the model. All the classes are expanded and grouped together through the connection equations generated automatically. The resulting code is hence composed only by equation, constants, variables and functions. The result of this first step is an implicit DAE system that could be extremely difficult to be solved

- **Analysis**

In this phase the "matching problem" is solved. The software check if it is possible

to assign one different unknown to each equation. For high index DAE systems, index reduction algorithms are applied. Then, If the DAE system is structurally nonsingular, equations can be sorted in data-dependency order. This allows solving several smaller DAE systems in cascade, rather than a single large DAE system, thus gaining efficiency. The sorting procedure is known as BLT-transformation, conversion of the structure incidence matrix of the DAE system into Block Lower Triangular form

- **Optimization**

In this phase trivial equations are removed and a tearing algorithm is applied. This necessity arise from the fact that we would like to express the problem as the smallest possible ODE or DAE system, and compute the values of all other variables from the solution of this minimal problem. However, the minimal set of equations depending on inputs and state variables only, is not the most efficient form in general. In fact, this implies often the unnecessary repetition of some calculations. By converting equations into assignments it is possible to avoid repeated computation, increasing the efficiency

- **Code Generation**

At the end of the previous step, a minimal set of differential equations and algebraic equations is obtained. In the fourth phase the C code is generated. This code will be used to perform the simulation model by linking this equations system to the numerical solver

- **Compilation**

At last the code generated in the previous point is compiled to produced an executable file for the simulation

6 | Model Reduction

In this chapter all the fluid simplifications and their consequences on the steady-state behavior of each component of the cycle will be discussed . In particular in the following sections will be presented three different types of models, one composed by pure CO₂, one composed by CO₂ and water and the last one composed by CO₂ and oxygen. Also a fourth case will be analyzed in the next pages, the one with pure CO₂ with oxygen tracking. This simplifications are applied to the system in order to decrease the overall complexity of the entire model and decrease its computational load. For each case a comparison with the real CO₂ mixture is made in order to evaluate the differences and select which are the most influential components inside the real mixture. Finally an entire model with different reduced fluids in different areas of the cycle will be presented, different reduced fluids are used to more precisely catch all the relevant contributions given by the species appearing in different part of the Allam cycle.

Since my work is based on the study of Muro Alvarado [19], who used PREOS to model the real fluid, I decided to use the same equations of state to model the reduced fluids. These equations of state were selected to model the fluid thanks to a work of Scaccabarozzi et al. [23] in which they developed an analysis comparing different state equations to verify the accuracy of CO₂-H₂O mixtures models, giving as a result that PREOS was the best solution.

This aspect is strictly connected to the core of my work. As already discussed in Chapter 4, simpler models implies a lower number of equations and this fact has a huge impact on the computational load of the simulations. Less equations means faster simulations that are much better from a control point of view, in particular this simplifications can lead to an easier design and implementation of the controllers.

6.1. Fluid Models

6.1.1. Real Mixture

The starting point of my thesis is the fluid used by Muro Alvarado [19] in its previous work. Its fluid is a complex mixture composed by 5 elements: CO_2 , O_2 , N_2 , H_2O and Ar . The most relevant contribution in the mixture is given by the CO_2 but in some specific parts of the cycle the contribution of other components affect a lot the total energy of the mixture. In particular, when the CO_2 is near the critical point, its density is affected by the other components, which are far from the critical point and therefore less dense. Another relevant phenomenon that need to be considered and affects a lot the mixture properties is the water condensation in the regenerator. A variation in the enthalpies is generated and the presence of H_2O in the fluid is quite relevant. Another point in which pure CO_2 is not enough is the oxidant stream, where the contribution given by the oxygen is not negligible. This fact led me to develop, not only the model of pure CO_2 , but also other specific fluid models to be applied in determined part of the cycle. All these models are described later in the chapter.

Considering the composition of the real fluid, the PREOS as state equations and the total complexity of the plant, the result is a final model composed by 110 000 equations and this, as already said in the introduction of the Chapter, is the reason why we need to simplify the fluid model.

6.1.2. Pure CO_2

There are parts of the cycle in which the concentration of the CO_2 is over 98% and there is no need to take into account the presence and the quantity of oxygen in the mixture or to consider the contribution given by condensed water. For these reasons a simpler model can be considered, in particular, in our case we approximated the real mixture with pure CO_2 . Thanks to this approximation, the complexity of the fluid model is widely reduced and consequently also the overall complexity of the cycle is directly reduced.

An important step to validate a model is to verify its reliability and accuracy with respect to the reality or as in our case with respect to the real mixture. In order to do so, I created different tests in which at specified pressures (low pressure, slightly supercritical and high pressure) and temperatures (sliding temperatures in a range of values) some of the main thermodynamic properties of the fluid are calculated (density, specific heat capacity, dynamic viscosity, specific energy, thermal conductivity, specific internal energy, specific enthalpy).

In figures 6.1–6.4 some results in the case of low pressure ($p = 1e5$ Pa, $T = [800-1500$ °C]) are reported, but the same results, analysis and observations are done also in other conditions. These experimental values are then compared with some reliable data, in our case the data obtained with the real mixture. From the graphs we can say that the error never exceeds the 5%, a value that for our modeling and control purposes can be accepted.

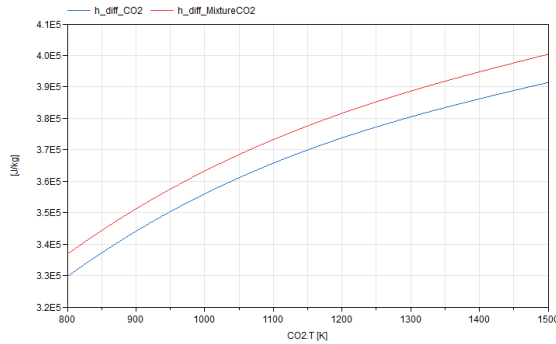


Figure 6.1: Specific enthalpy

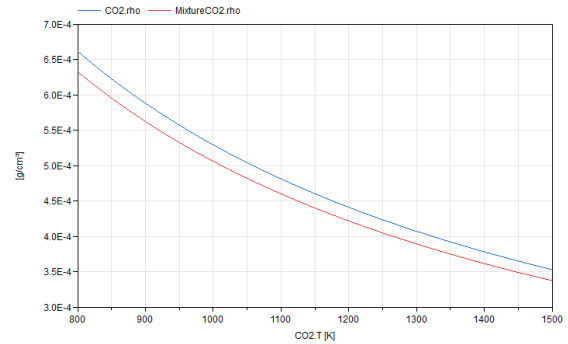


Figure 6.2: Density

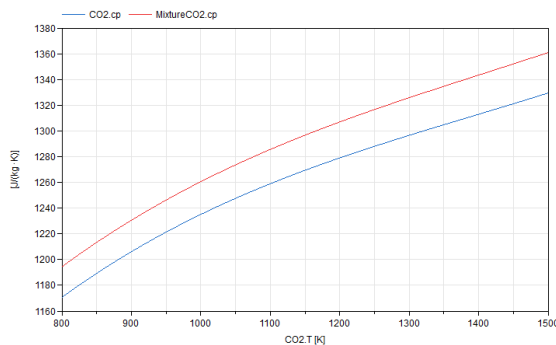


Figure 6.3: Specific heat capacity

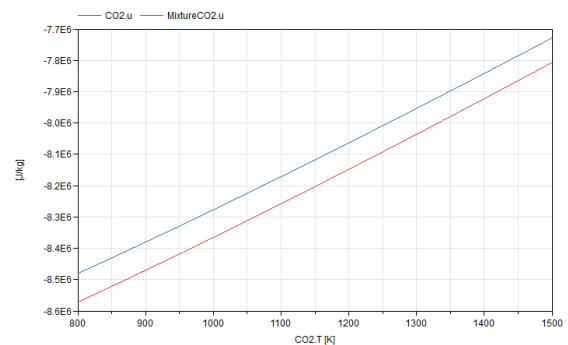


Figure 6.4: Specific internal energy

6.1.3. CO₂+ Water

Another model that we decided to apply in some parts of our plant is the one composed by CO₂ and water. In this case, being composed by two species, the model should be more reliable with respect the one composed by pure CO₂, this because it is more similar to the real mixture. In particular, by adding the water to the mix, we are now able to take into account its contribution that in some cases is really relevant and cannot be neglected. An example could be the outlet stream of the turbine or of the combustor, where, due to the phenomenon of water condensation, the enthalpy contribution given by the water is huge and affects a lot the fluid properties. Last thing that I want to stress is the fact that in this case, we are not talking anymore about a pure substance as in the case of the pure CO₂ but we are talking about a mixture, composed by two elements. The direct effect of

this fact is that during the simulations with this fluid model, the computational load will be bigger than the one in the case of pure CO_2 .

Looking at the results in Fig. 6.5–6.8, we can observe that the obtained results are very good, the maximum error is around 0.5%.

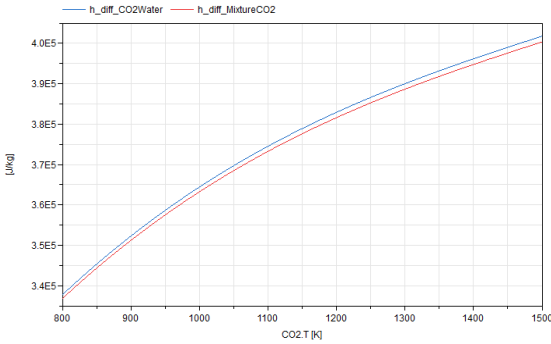


Figure 6.5: Specific enthalpy

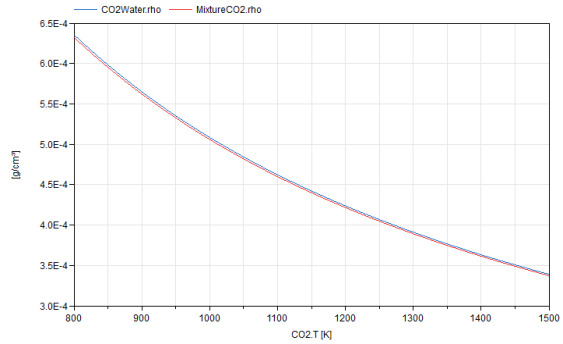


Figure 6.6: Density

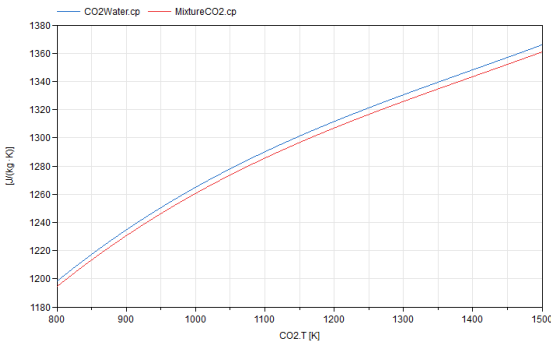


Figure 6.7: Specific heat capacity

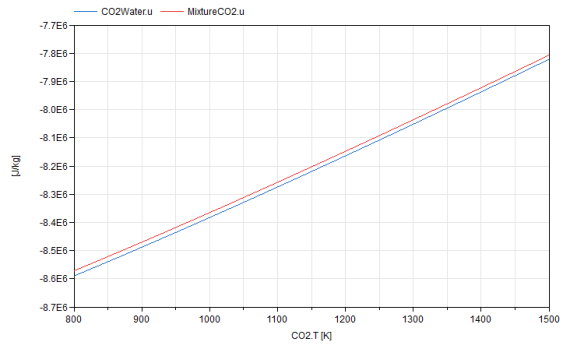


Figure 6.8: Specific internal energy

6.1.4. CO_2 + Oxygen

The third model here presented is the one composed by CO_2 and oxygen. As the previous model, it is composed by two species, for that reason we expect that its behavior will be much more similar to the one of the real mixture with respect the one of pure CO_2 and also its computational load will be bigger respect to the one of the fluid model with a single component. We thought to try this model in order to take into account the contribution given by the oxygen in particular parts of the cycle, in the specific case at the end of the compression stage, when the oxidant stream is created, mixing practically pure CO_2 with oxygen. In this situation the percentage of oxygen present in the mixture is around the 10%, a quantity that could give a significant contribution to the fluid model.

As can be observed in Fig. 6.9–6.12, the results of this model are pretty different, some variables are well represented, for example the density, where the error is less than the

1%, some other are very different, for example the specific heat or the internal energy, where the error can reach the 10%.

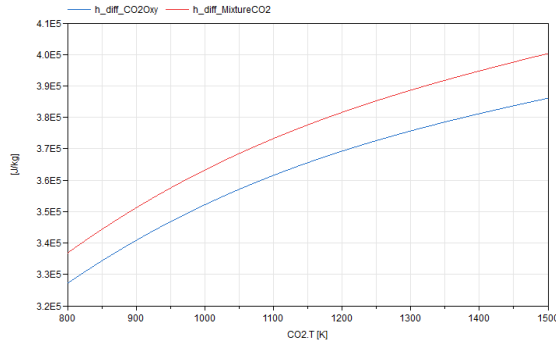


Figure 6.9: Specific enthalpy

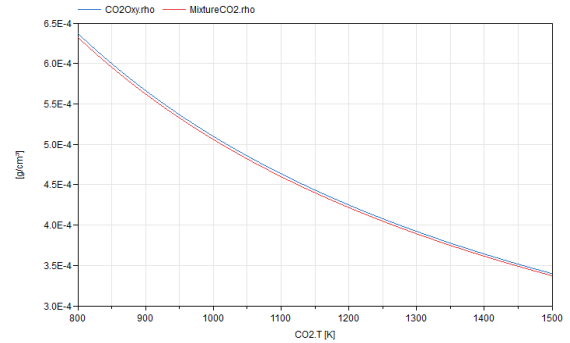


Figure 6.10: Density

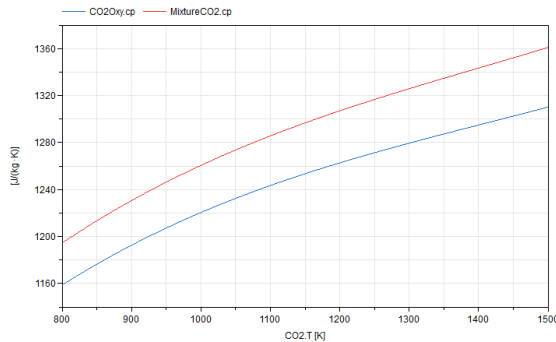


Figure 6.11: Specific heat capacity

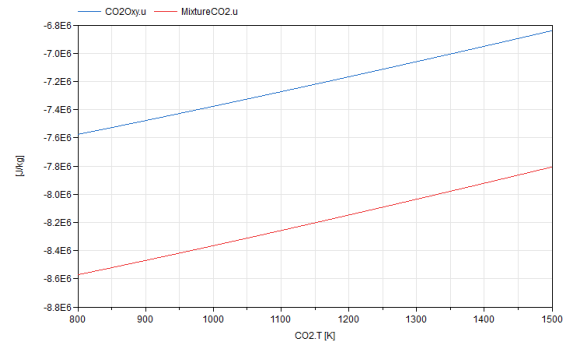


Figure 6.12: Specific internal energy

6.1.5. Oxygen Tracking Model

Finally, another attempt that I did is to create a particular model in which the thermodynamic properties of the fluid are calculated using pure CO_2 but a tracking component for the quantity of oxygen along the cycle is added. This model is based on the idea to take the best from two different models. The light computational weight from the pure CO_2 model and the ability to know the percentage of oxygen in every part of the cycle from the model composed by $\text{CO}_2 + \text{Oxygen}$. This second aspect may seem not important but the quantity of oxygen in the mixture is fundamental in the control strategy, in which this variable is one of those to be controlled and thus its measurement is needed. In this case there are no tests because of the fact that the thermodynamic variables are computed using pure CO_2 and the graphs would be the same that can be observed in section 6.1.2.

6.1.6. Comparison

In this section all the fluid models (real mixture included) will be compared each other. The test is the same type of the one already discussed in the previous section 6.1.2, in this case applied to all the four models. During the analysis, the reference graphs that will be taken into account are the ones that refers to the specific enthalpy difference (due to its relevant contribution on important variables for the efficiency of the cycle, such as the turbine outlet temperature, combustor outlet temperature and the electrical power) but the same behaviours and results are obtained also for other variables such as specific heat capacity, specific energy, etc.

As can be observed from the figures 6.13, 6.14 and 6.15, the most reliable model, as expected, is the one composed by CO₂ and water, this is because it is the most similar to the real mixture but being composed by two element it is also more computational demanding than a model composed by one specie. The model composed by pure CO₂ is the simpler one but it also presents a bigger error with respect to the previous model and to the real mixture. In this case, even if the error is bigger than the one in the CO₂ + water model, it is still acceptable and will not create any problem.

It is important to notice the behaviour of the model composed by CO₂ and Oxygen. Even if it is composed by two species and theoretically should be more realistic than the one composed by pure CO₂, the error with respect the real mixture is larger. This particular behaviour, even if the error is not huge (about 10% in the worst case), could create problems in the plant when used in turbo-machines, affecting the overall results of the entire cycle. These observations will be performed in the last section of this chapter (section 6.7).

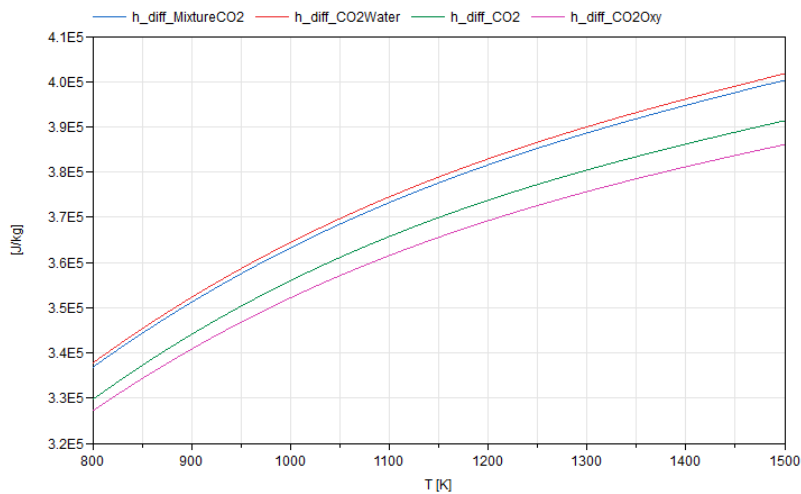


Figure 6.13: Enthalpy difference at low pressure ($p = 1e5$, $T = [800-1500 \text{ }^\circ\text{C}]$)

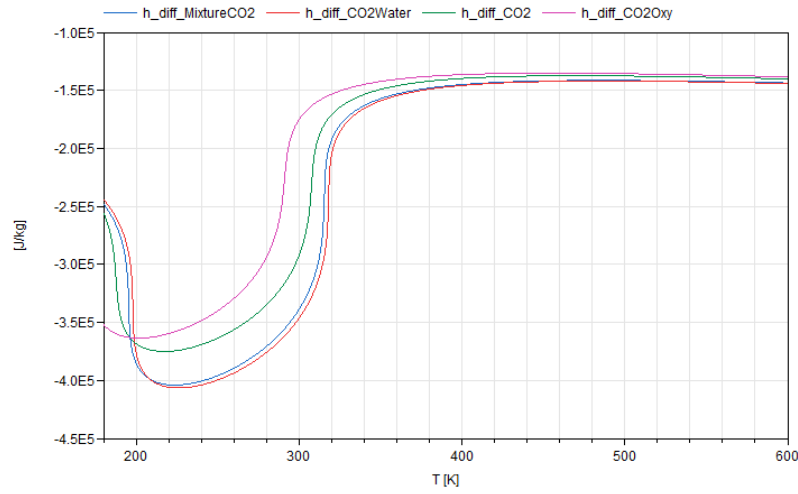


Figure 6.14: Enthalpy difference at supercritical conditions ($p = 80e5$, $T = [180-620 \text{ }^\circ\text{C}]$)

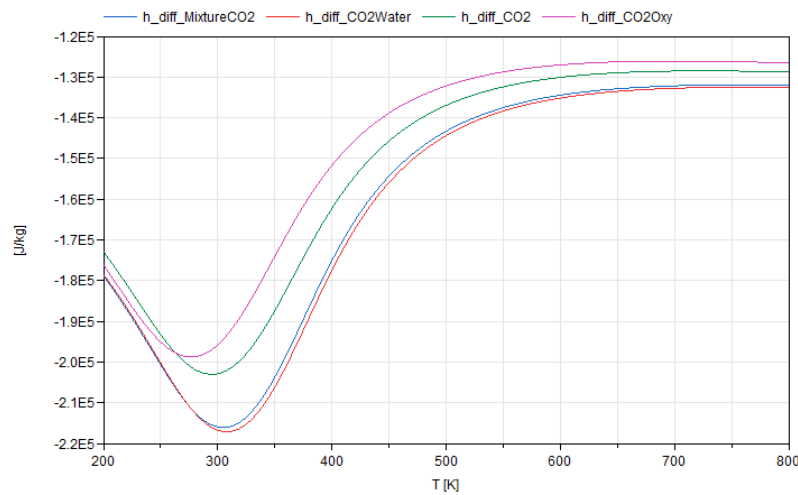


Figure 6.15: Enthalpy difference at high pressure ($p = 300e5$, $T = [200-800 \text{ }^\circ\text{C}]$)

The overall scheme that came from our analysis is the one in figure 6.19. As can be observed, all the streams after the Water Separation Unit (WSU) and before any mixing with oxygen or super-heating (low-pressure part of the cycle), are approximated as pure CO_2 . This is possible because in all these streams the percentage of CO_2 is over 98% and for that reason the contribution of all the other species is considered negligible. The fluxes coming from the mixture between CO_2 and oxygen (oxidant streams) are approximated as $\text{CO}_2 + \text{oxygen}$ to take into account the contribution given by the oxygen. In the streams coming from the combustion chamber outlet and the turbine, a fluid model composed by CO_2 and water is used. This model is able to take into account the huge contribution given by the water in that part of the cycle, in particular the contribution given by the condensed water that cannot absolutely be neglected.

Finally, in figures 6.16–6.18 can be observed the comparison of some thermodynamic properties at different pressures. It is interesting to verify what we already discussed in the section dedicated to the thermodynamic properties of the supercritical CO_2 (section 2.1.1). Despite the errors between different fluid models, the general behavior, particularly of the specific heat and of the density, respects what we expected and we knew from the theory, confirming the correctness of our models.

A last comment can be done on the model composed by pure CO_2 + oxygen tracking. This model has not been taken into account into the analysis because as already said in 6.1.5, its thermodynamic properties are calculated as if it were composed by pure CO_2 , and we would have obtained the same results of the easiest model. This model can be used in every stream where the CO_2 + oxygen model is used, decreasing the computational load of the simulation but neglecting the contribution given by the oxygen, taking anyway trace of its quantity. Later in the thesis its applicability in the cycle and the obtained results will be discussed (Chapter 7).

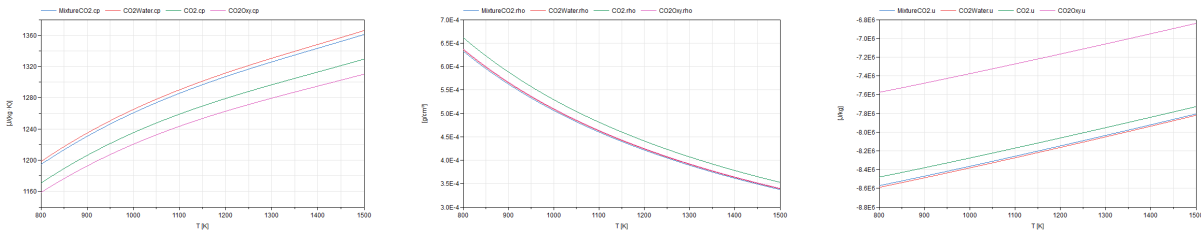


Figure 6.16: Test at low pressure conditions (C_p, ρ, u)

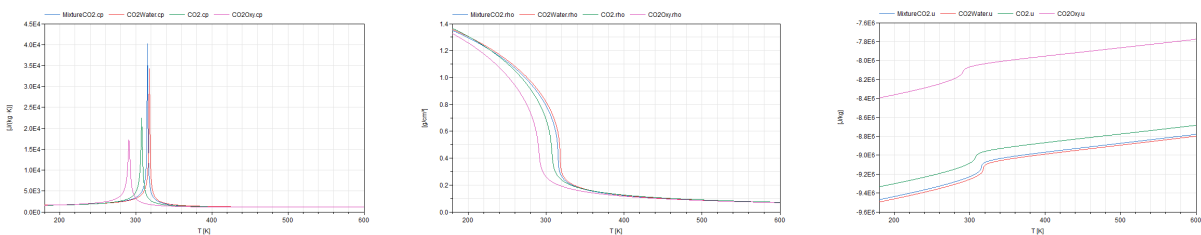
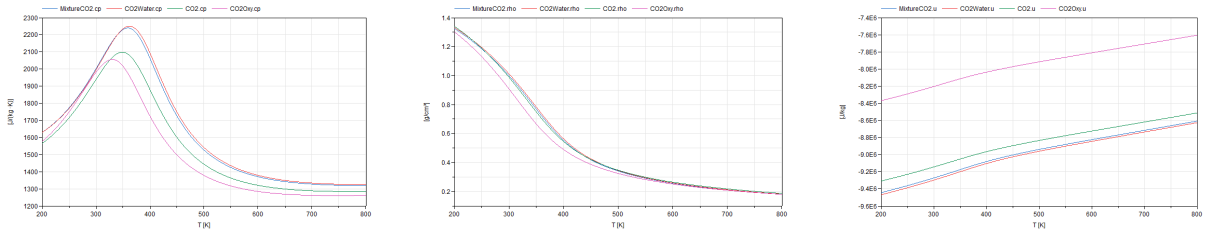


Figure 6.17: Test at slightly supercritical conditions (C_p, ρ, u)

Figure 6.18: Test at high pressure conditions (C_p, ρ, u)

6.2. Compression System

In this section we consider the turbo-machines present in the cycle, in particular we will discuss about the behavior of the compression system of the cycle when reduced fluids are applied. In this particular case, being the percentage of CO_2 more than the 98% in every part of the subsystem, the real fluid is approximated as pure CO_2 . The subsystem is composed by a set of four compressors and four intercoolers (Fig. 6.20). The model of a single compressor developed by [19] is based on mass and energy balances (appendix A) and also by the characteristic map given by Zayrab [25]. The intercoolers are modeled as counter-current heat exchangers, thus, the same modelling techniques that will be shown for the regenerator (6.6) are used also here. The main difference is that the cold fluid for the intercoolers is liquid water, working at temperatures between 25°C and 50°C and from 1 to 2 bar.

Each compressor has been tested individually but similar results have been obtained, for that reason in 6.1 and 6.2 can be observed the results of the entire compression system of the plant. The test is composed by an ideal pressure source connected to the inlet of the first compressor and an ideal mass flow sink connected at the outlet of the fourth compressor. The variables considered in the comparison are the outlet temperature, which is the most important one since after each compressor there is an intercooler, and the outlet density of the gas in order to be sure to work in with the right conditions and exploit the properties of s- CO_2 discussed in 2.1.1, reducing the compression work.

Looking at the results in 6.1 and 6.2 we can observe that the error of the outlet temperature (T_{out}) is below the 1%. This confirm the choice made for the simplified fluid used in the compression system, pure CO_2 is able to represent the main energy contribution given by the real fluid. Looking at the densities we can see that the error increase for each compression stage until an error around the 5%. This result can be explained by the fact already observed by [19] in its work during the validation of its real fluid model, the error increases approaching to the liquid state. The error is still acceptable and we can conclude that it is possible to use pure CO_2 to simplify the fluid in the compression system.

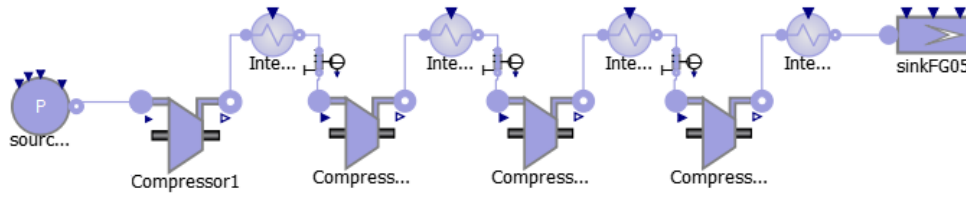


Figure 6.20: Compression system test model

Compressor	Real Mixture		Reduced Fluid		Error %	
	T_{out}	ρ_{out}	T_{out}	ρ_{out}	ΔT_{out}	$\Delta \rho_{out}$
	°C	kg/m ³	°C	kg/m ³	%	%
C1	47.74	74.93	47.67	75.88	-0.15	1.27
C2	46.26	105.17	46.26	106.87	0.00	1.62
C3	46.99	151.51	47.05	155.00	0.13	2.30
C4	48.13	234.76	48.34	244.48	0.44	4.14

Table 6.1: Compression system results (T - ρ)

Compressor	Real Mixture		Reduced Fluid		Error %	
	P_{in}	P_{out}	P_{in}	P_{out}	ΔP_{in}	ΔP_{out}
	bar	bar	bar	bar	%	%
C1	29.07	37.80	29.07	37.80	0.00	0.00
C2	37.61	48.90	37.61	48.90	0.00	0.00
C3	48.68	63.30	48.68	63.30	0.00	0.00
C4	63.14	82.10	63.14	82.10	0.00	0.00

Table 6.2: Compression system results (ΔP)

6.3. Pumping System

In this section we will analyze the behaviour of the pumping system present in the cycle when the reduced fluid is applied. the model of a general individual pump is done following the general characteristics of this turbomachine and the specific characteristics given by

Zaryab, Scaccabarozzi, and Martelli [26]. The equations for the mass balance, energy balance and isentropic efficiency are equal to the ones used for the compressor model (section 6.2). As can be observed in Fig. 6.21, in the system three pumps are present, two used to control the mass flow rates (pump6 and pumpOxy) and one used to control the pressure (pump5), thus we have two different pump models that are practically the same but differs only in the input or in the manipulated variable of the component.

To compare the results we use as test model our entire pump system with a prescribed pressure source at the inlet of the first pump (Pump5) and another prescribed pressure sink at the outlet of both Pump6 and PumpOxy (Fig. 6.21).

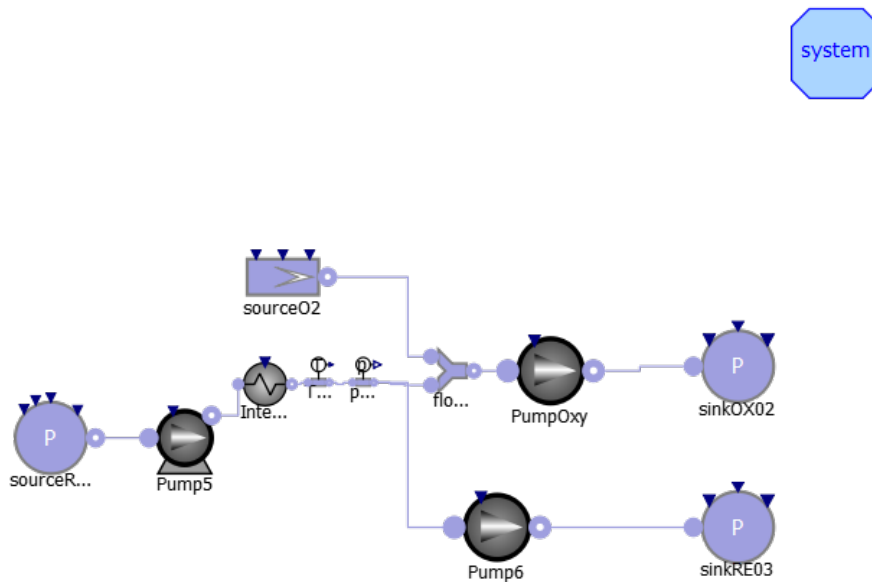


Figure 6.21: Pumping system test model

In the same figure we can observed the input and output streams of the subsystem. One input stream is the pure CO_2 fluid coming from the compression system, the other one is the pure O_2 stream used to create the oxidant stream. The output stream of "PumpOxy" (oxidant stream) is mainly a mixture of oxygen and CO_2 , for that reason, as discussed in 6.1.6, I decided to model it with a $\text{CO}_2 + \text{oxygen}$ model. On the other side, the outlet stream of "Pump6" (recycle stream) is the same coming from the compression system and can be simplified as pure CO_2 without losing information.

We can conclude this section by looking at the results in Fig. 6.3. In general the results in Pump5 and Pump6 are acceptable and the maximum error is the one on the outlet temperature of "PumpOxy" that is around the 18%. This is not a strange result because we already observed in 6.1.4 that the errors in this model composed by CO_2 and oxygen are the greatest between all the fluid models. This error can be caused by a too strict

simplification of the fluid present the pump that is no more able to well represent the properties of the real fluid. Despite that, we can still maintain the same simplification and analyze the consequences caused by this choice later in the thesis (section 6.7) where closed cycle steady-state analysis will be performed. That point only we will evaluate if this error affects too much the overall plant model reliability or not.

Pump	Real Mixture		Reduced Fluid		Error %	
	T_{out}	P_{out}	T_{out}	P_{out}	ΔT_{out}	ΔP_{out}
	°C	bar	°C	bar	%	%
Pump 5	35.08	121.25	34.66	125.47	-1.2	3.48
Pump 6	55.94	312.10	52.05	312.10	-6.95	0.01
Pump Oxy	53.09	312.10	43.59	312.10	-17.89	0.01

Table 6.3: Pumping system results

6.4. Combustor

In this section the behavior of the combustor with reduced fluids will be analyzed. The first thing to underline is the fact that the fuel model is the same of the work of [19], in particular it is a mixture of multiple components with prevalence of CH_4 modeled as the real CO_2 mixture with PREOS. The combustor is modeled as a 0D model, including the classical definition for dynamic mass and energy balances (appendix A). Additionally, it is important to consider a partial mass balance equation, taking into account the chemical reaction that occurs in this equipment.

The combustor in the cycle has 3 input streams (fuel, oxidant, recycle) and 1 output stream (flue gas). The fuel, as already said here above, is the complete mixture not approximated. The oxidant stream is the flux coming from the pump P_{oxy} , and the recycle stream is the flux coming from pump P6. For this reason these streams are approximated as the fluxes coming from the respective pumps described in section 6.3. The outlet stream, due to the chemical reactions in the combustor, contains water vapour, whose enthalpic contribution cannot be neglected, and for this reason a model composed by CO_2 and water (6.1.3) is the best choice.

The model is tested considering ideal pressure and mass flow rate sources and/or sinks connected in each of the interfaces. In our case three ideal mass flow rate sources, representing the inlet of the oxidant, recycle and fuel streams and one pressure sink, representing a sink of flue gas are used (Fig. 6.22).

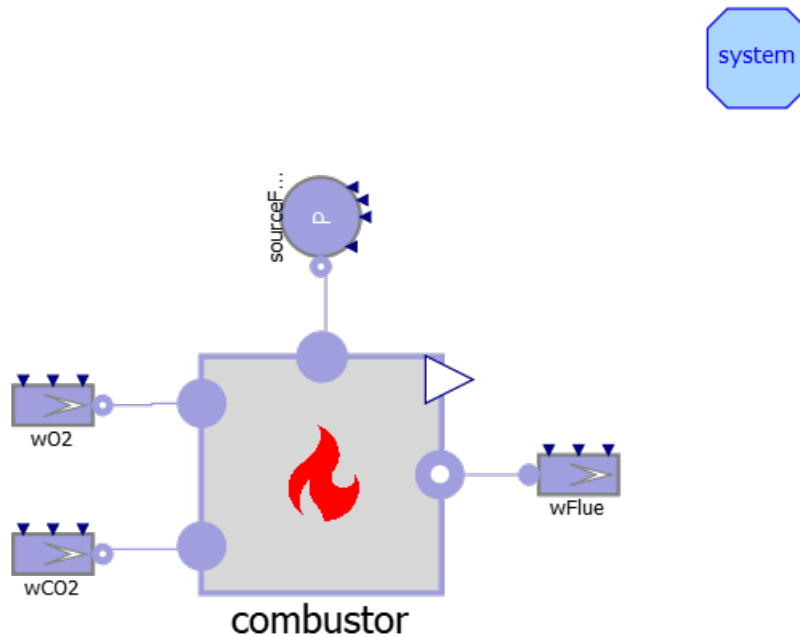


Figure 6.22: Combustor test model

The values of temperature, density and specific enthalpy obtained using reduced fluid models will be compared with the ones obtained with the real mixtures. In table 6.4 both the values of these variables can be observed, the obtained errors are abundantly below 1%. This confirms the fact that, although different fluids, simplified in different ways are mixed in the combustor, the relevant contributions of each stream is still taken into consideration and the model is still realistic.

Combustor Flue Gas	Unit	Real Mixture	Reduced Fluid	Error %
Temperature	°C	1154.80	1157.20	0.21
Density	kg/m ³	102.35	102.66	0.30
Specific Enthalpy	Mj/kg	-7.596	-7.611	0.20

Table 6.4: Combustor results

6.5. Turbine

In this section the behavior of the turbine will be discussed. The turbine model of the Allam cycle is a particular one, for our modelling purposes, it has been assumed that the turbine will have only two stages and the total cooling flow will enter between these two (Fig. 6.23).

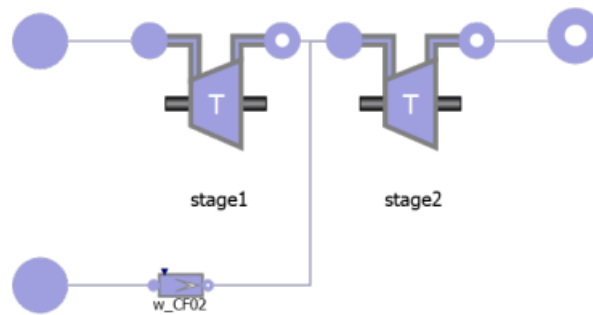


Figure 6.23: Turbine 2 stages

This cooling flow (moderator stream, pure CO_2) is needed to cool down the flue gas stream coming from the combustor because of its high temperature that could damage the turbine. This model is based on the model created by the Department of Energy of Politecnico di Milano that developed a turbine model that can cover the static requirement of the process. This model is based on the El-Masri's continuous expansion model [14].

In our case the turbine has two input streams and one output stream. One input stream is the flue gas at high temperature coming from the combustor and the other one is the moderator flux coming from the regenerator. The only outlet stream is the flue gas leaving the turbine. The flue gas streams composition is the same of the outlet stream of the combustor, for this reason, as in combustor section (6.4), are simplified as $\text{CO}_2 + \text{water}$. The moderator stream, being the same stream coming from pump6 (6.3), is simplified as pure CO_2 .

In order to validate the model, the test (Fig. 6.24) is done connecting to each input a source pressure or mass flow rate and to each output a sink of the same type. The variables analyzed are the electric power and the Turbine Outlet Temperature (TOT) not only at nominal conditions but also in part load down to 50% of the thermal load. From 6.5 we can observe that the errors in the temperatures are all below the 1%, the errors related to electrical power increase as we go to lower loads, but the maximum is the one at nominal conditions. These differences are still below the 1.5%, that is an acceptable value for our control purposes.

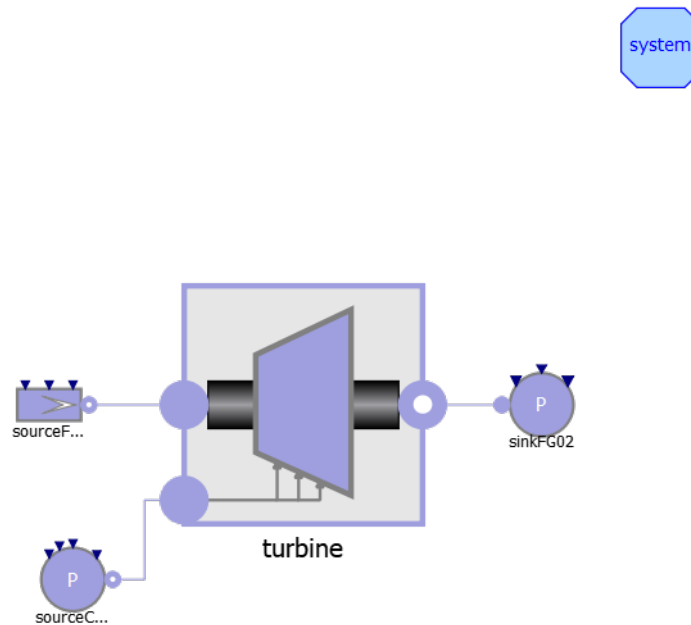


Figure 6.24: Turbine test model

Turbine Load %	Real Mixture		Reduced Fluid		Error %	
	P_e MW	T_{out} °C	P_e MW	T_{out} °C	ΔP_e %	ΔT_{out} %
100	612.32	725.02	620.01	724.42	1.25	-0.08
90	550.91	720.11	553.42	713.02	0.45	-0.98
80	490.11	717.54	492.76	710.40	0.54	-1.00
70	429.53	716.84	432.02	709.7	0.58	-1.00
60	367.98	716.22	370.32	709.16	0.64	-0.99
50	304.34	713.13	306.54	706.34	0.72	-0.95

Table 6.5: Turbine results at different loads

6.6. Regenerator

Hereinafter the model and the behavior of the regenerator of the cycle when reduced fluids are applied will be discussed. In particular in the first subsection will be described the model of a single heat exchanger and in the second one the entire regenerator "specialized" for this particular plant. As already said in 6.1.6, this is a crucial component for the cycle because the overall efficiency of the plant depends on its efficiency. This is why it is also

important to create a reliable and accurate model using simplified fluids.

6.6.1. Heat Exchanger

In the regenerator there are several heat exchangers working together with connected streams, thus, it is necessary to develop the model of a single heat exchanger (Fig. 6.25). The function of the heat exchanger is to transfer heat between two or more fluids depending on the direction of the flows going through, it can be classified in parallel flow, counterflow and cross flow heat exchanger. It is important to have a representation of a control volume with compressible fluid as working fluid that can be exposed to a heat flow.

The continuous total volume is approximated as a discrete one, composed by N control volumes delimited by $N + 1$ nodes. Every control volume is represented by a lumped parameter model with dedicated boundary conditions. The degree of approximation depends on the numbers of finite volumes chosen which also influences the computational complexity, then it is important to make a trade-off between this relationship [19]. ThermoPower Library [11] contains the used Flow1DFV model which represents this control volume under specified assumptions.

At this point, to model the heat exchanger, mass, momentum and energy balance equations are applied, with the only difference that now these equations need to be written for each control volume (appendix A). This is the reason why increasing the number of control volumes increases also the computational complexity.

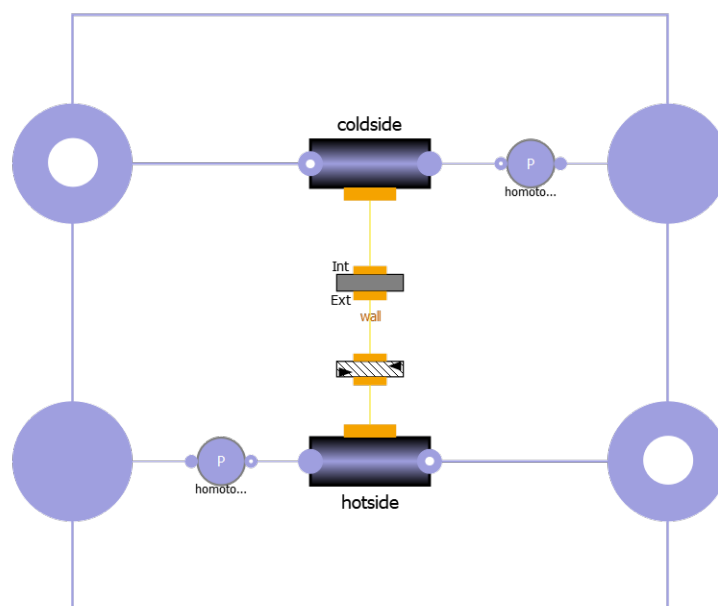


Figure 6.25: Heat exchanger model block

6.6.2. Regenerator Model

In this section we will analyze the specific regenerator of this plant and its behavior with reduced fluid but before that, an analyses of its structure is needed. The regenerator is a set of 12 counter-current heat exchangers (Fig. 6.26), which are divided into five modules, based on the working temperature along each module. Incoming and outgoing flows for each module are approximated differently, the simplified model choice for each stream is done relying on the considerations in the previous sections. This is possible thanks to the fact that all the fluxes present in the regenerator are coming from the pumps or from the turbine, whose simplified models are already described in their respective sections 6.3 and 6.5. The only different stream in the regenerator is the one coming from the ASU, which is air and is the same mixture used by [19] in its previous work. Each module will be described here below:

- High Temperature Module:** In this level there are two heat exchangers, HX01 and HX02. The flue gas coming from the turbine enters into the regenerator and is split between the two heat exchangers working as the hot fluid. This flux, being the flue gas coming from the turbine is simplified as $\text{CO}_2 + \text{water}$. On the other side, there are two cold fluids, the first one is the one coming from pump Poxy and going through HX01 and the second one is the fluid coming from pump6 and going through HX02. As already described, the fluid coming from pumpOxy (oxidant) is simplified as $\text{CO}_2 + \text{oxygen}$ and the other (recycle stream) as pure CO_2 . In nominal conditions, the temperature of the cold sides goes from 519°C to 705.4°C .
- Medium Temperature Module:** In this level there are two heat exchangers HX03 and HX04. The flue gas ($\text{CO}_2 + \text{water}$) goes through the heat exchangers in the same way as the previous module, entering with a temperature of 550°C and exiting with 272.8°C . The cold fluids that go through HX03 and HX04 corresponds to the same fluids going through HX01 and HX02 respectively. The temperature in the cold side goes from 248.4°C to 519°C .
- Low Temperature Module:** In this module there are three heat exchangers: HX05, HX06 and HX07. The flue gas coming from the medium temperature module ($\text{CO}_2 + \text{water}$) goes through these three heat exchangers, reducing its temperature from 272.8°C to 113.8°C at the outlet. On the contrary, now there are three cold fluids, one per each heat exchanger: in HX05 the cold fluid corresponds to the one coming from the pumpOxy ($\text{CO}_2 + \text{oxygen}$) which later goes to HX03 and HX01; in HX06, the cold fluid is part of the stream from the recycle stream (pure CO_2) and finally in HX07, the cold fluid is the moderator (pure CO_2) that after this

heat exchanger, goes to the turbine. The temperatures of the cold fluids goes from 109.1°C to 248.4°C.

- **Low-Low Temperature Module:** In this level all the cold fluids enter the regenerator, the one coming from the pumpOxy (CO_2 + oxygen) enters into HX08, the flow corresponding to the recycle stream (pure CO_2) goes partially through HX09 and partially through HX12 and the moderator stream (pure CO_2) enters to HX10. This is the inlet point of all the cold streams that later will go through the others heat exchangers located in the previous levels.
- **Air Hot Fluid Module:** This module is composed by two more heat exchangers HX11 and HX12 that uses air coming from the ASU as hot fluid, exchanging heat with the rest of the recycle stream (pure CO_2).

In figure 6.26 can be observed the overall regeneration system of the cycle.

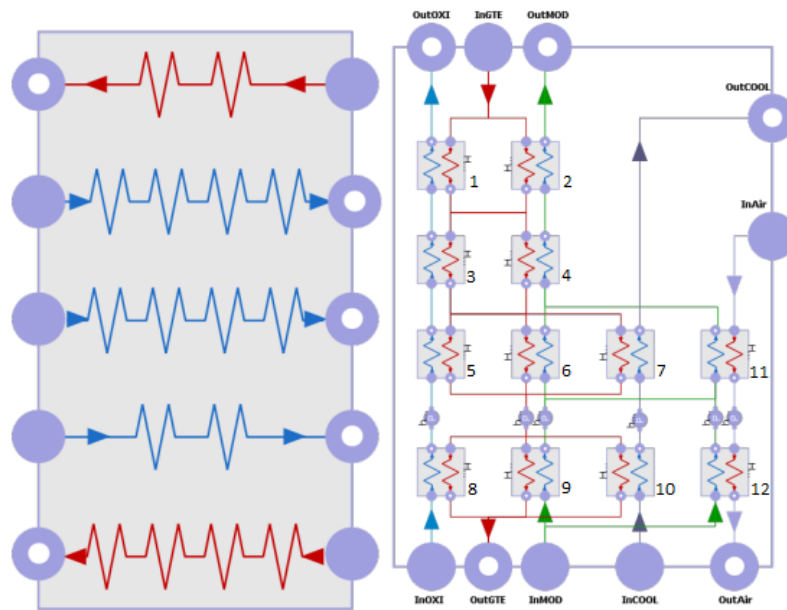


Figure 6.26: Regenerator model

In this last part of the section the results obtained with the regenerator with the real mixtures and the ones with the reduced fluids will be compared. The basic parameters to be evaluated and compared are the temperature difference between inlet and the outlet of the hot and cold sides. The basic test model of the regenerator is shown in figure 6.27 with one ideal prescribed pressure source at each inlet stream and one ideal prescribed mass flow at each outlet stream. From the table in 6.6 we can observe that the final outlet temperature errors of each stream, are all under the 1% except for the temperatures related to the cooling and flue gas streams. These differences are obviously due to the fact

that the fluids have been simplified and now they are no longer able to 100% catch the contribution given by each component and consequently the behavior of the real mixture. Given that, we are talking about temperature differences of hundreds of degrees kelvin, for this reason an error of 10 degrees (that could be considered high in general), in our case is good enough for our modelling and control purposes.

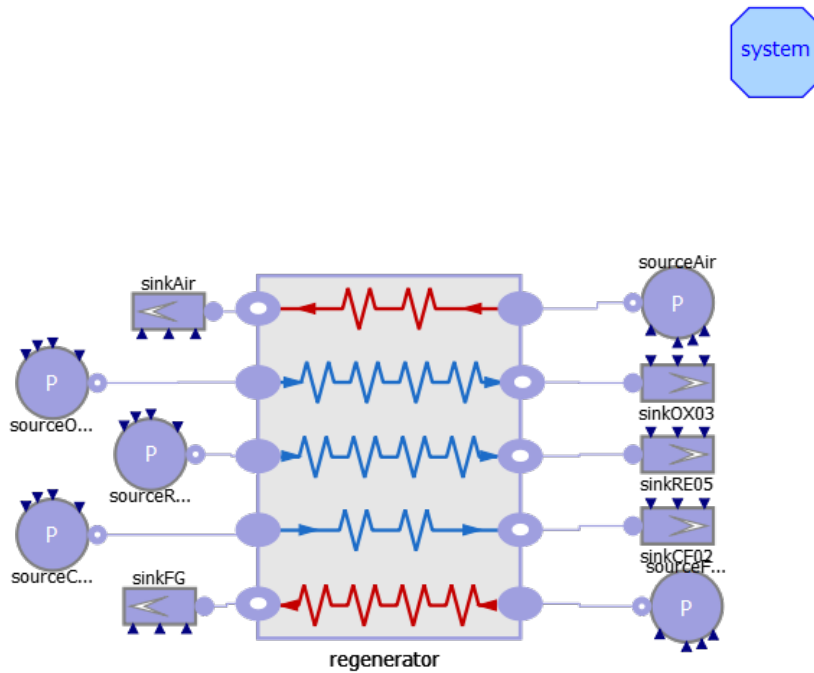


Figure 6.27: Regenerator test model

Regenerator	Real Mixture		Reduced Fluid		Error %	
	h_{out} Mj/kg	T_{out} °C	h_{out} Mj/kg	T_{out} °C	Δh_{out} %	ΔT_{out} %
Oxidant	-7.21	705,72	-7.21	703.22	0.05	-0.35
Moderator	-8.09	705,42	-8.13	702.92	0.49	-0.35
Cooling	-8.84	148,68	-8.92	136.21	0.90	-8.39
Flue Gas	-8.98	62,30	-8.99	59.48	0.11	-4.53

Table 6.6: Regenerator results

6.7. Allam Cycle Reduced Model

In this final section the steady state behavior of the closed plant when reduced fluids are applied will be discussed. At this point the only thing to do is to connect, as presented in figure 6.19, all the components that have been described here above. In the same figure, the reduced fluid applied in each part of the cycle can also be observed. The main variables to be verified are the ones already described in each component section but the most important are those most influential on the efficiency of the cycle, that are the ones related to the high pressure part of the cycle (combustor outlet temperature, turbine outlet temperature and the produced electrical power).

The results can be observed in the tables at the end of the section. Looking at the data we can say that they have more or less the same order of magnitude than the ones obtained in the individual component tests and are acceptable for our control purposes. As imaginable from the observations made in 6.1.6 and 6.3, regarding the PumpOxy outlet temperature, which is the biggest error between all the variables, we can now say that even if its value is not so close to the real one (about 20% error, table 6.8), it does not affect the other important variables, the ones related to the turbine, combustor and regenerator, for that reason we can keep this fluid model for the oxidant stream. We can finally conclude that at the steady-state, all the model simplifications are able to replicate the real behavior of the system without loss of information for the purposes of control design.

At this point we can try to give also some information about the complexity of the system. As already described in chapter 4, the computational weight of a model largely depend on the number of equations that need to be solved. A purpose of my work is also to evaluate if could be possible to decrease this number of equations maintaining the reliability of the model. The closed cycle model with the real fluid has about 100 000 equations, the one with the simplified fluids has about 45 500 equations, which are less than a half of the starting number. As predicted, the simulation time is also decreased, it passed from failing the simulation due to lack of memory after 5 minutes of computations in the real case to one minute and a half, without errors, in the simplified one, both cases using the same standard personal computer (i5 10th generation with 8GB ram). Finally we can also say that the work worth it because we managed to simplify the model without losing the reliability of the previous model.

Compressor	Real Mixture		Reduced Fluid		Error %	
	T_{out} °C	ρ_{out} kg/m ³	T_{out} °C	ρ_{out} kg/m ³	ΔT_{out} %	$\Delta \rho_{out}$ %
C1	47.68	75.03	46.26	76.60	-2.98	2.09
C2	46.63	104.00	46.49	105.88	-0.30	1.81
C3	46.97	148.56	47.05	152.19	0.17	2.44
C4	46.55	232.53	46.66	243.82	0.24	4.86

Table 6.7: Closed-cycle compression system results

Pump	Real Mixture		Reduced Fluid		Error %	
	T_{out} °C	P_{out} bar	T_{out} °C	P_{out} bar	ΔT_{out} %	ΔP_{out} %
Pump 5	35.94	119.13	35.44	120.93	-1.39	1.37
Pump 6	55.15	312.84	52.09	312.74	-5.55	-0.03
Pump Oxy	52.42	312.53	38.74	312.43	-26.10	-0.03

Table 6.8: Closed-cycle pumping system results

Combustor Flue Gas	Unit	Real Mixture	Reduced Fluid	Error %
Temperature	°C	1156.22	1157.25	0.09
Density	kg/m ³	102.26	102.66	0.39
Specific Enthalpy	Mj/kg	-7.595	-7.613	0.24

Table 6.9: Closed-cycle combustor results

Turbine Load %	Real Mixture		Reduced Fluid		Error %	
	P_e	T_{out}	P_e	T_{out}	ΔP_e	ΔT_{out}
	MW	°C	MW	°C	%	%
100	619.06	726.19	620.63	725.37	0.25	-0.11

Table 6.10: Closed-cycle turbine results

Regenerator	Real Mixture		Reduced Fluid		Error %	
	h_{out}	T_{out}	h_{out}	T_{out}	Δh_{out}	ΔT_{out}
	Mj/kg	°C	Mj/kg	°C	%	%
Oxidant	-7.21	707.29	-7.21	705.042	0.01	-0.26
Moderator	-8.09	707.06	-8.12	705.33	0.37	-0.24
Cooling	-8.84	150.96	-8.88	143.38	0.45	-5.02
Flue Gas	-8.97	67.34	-9.00	56.86	0.33	-15.56

Table 6.11: Closed-cycle regenerator results

7 | Open-Loop Responses

The results obtained in the previous chapter only refer to steady-state simulations of the components and of the entire plant. To design the control strategies, it is important to also evaluate the dynamical behavior of the system. For this reason the aim of this chapter is to analyze the dynamical behavior of the cycle when reduced fluid are applied and compare the obtained results with the ones obtained with the real mixture. In order to do so, I applied some steps to specified input variables of the system, analyzing the response and the evolution of the output variables. No controllers are applied to the system, for this reason this analysis is considered as an open-loop analysis.

Before discussing the possible variable coupling, it is important to underline which are the variables involved in the process and in our analysis.

This process is a thermodynamic power cycle that produces electrical power from thermal power. From this definition, it is straightforward to understand that the electric power is the most important variable to be considered. In particular, a more complete and relevant variable to be considered is the net power produced by the plant (7.1). This variable takes into account also the power used by the compression and pumping systems, giving more realistic information about the efficiency of the cycle.

$$P_{net} = P_{turbine} - P_{pump} - P_{compressor} \quad (7.1)$$

Another fundamental variable for the efficiency of the plant is the TIT. As already described in the previous chapter, the turbine of the cycle was specially designed for this system, and its inlet temperature must be taken under control in order to avoid mechanical damages and maintain the efficiency. In this case the TIT cannot be directly measured due to the working conditions (too hot), for that reason it needs to be estimated by a model or directly the TOT can be used in the control scheme. On the same side of the process, another important variable to be considered is the composition of the flue gas, in particular the quantity of oxygen. This variable is important because it allows us to understand whether or not the combustion is performing well or not. Maintain the composition of O_2 to a prescribed value is important not only for the combustion, but

also for the compression system, because an excess of O_2 in the fluid could decrease the density of the CO_2 and as consequence the efficiency of the subsystem.

The efficiency of the compression system largely depends on the density of the CO_2 , for this reason it is important, in every working condition, to maintain the right pressure before the compression system and the right temperature before and after each compressor, where the CO_2 must work close to its critical condition. Finally, to create the oxidant stream, a stream of pure O_2 is mixed with a stream of CO_2 and in order to avoid a two-phase stream of O_2 , the pressure of the oxygen at this point must be 120 bar, then this variable must be considered in the analysis as well [19].

This procedure is important in order to better pair one manipulated variable with the respective controlled one. This can be done by a recursive approach, in which each possible scenario is analyzed, applying to each input variable a step and looking which is the most affected between all the output variables and finally, if possible, pair one manipulated variable with the controlled one. Before to choose a possible coupling configurations, it is useful to understand which are the most important variables of our plant.

The closed system can be divided into two subsystems: the hot side or high-pressure side, that includes the cold streams of the regenerator, the combustor, the turbine and all the variables related to them; and the cold side, or low-pressure side, that includes the hot stream of the regenerator, the condenser, the compression system and the pumping system.

For the high-pressure side the control objectives are:

- Meet continually the net power demand
- Maintain the turbine operation safe and efficient, this means, keep the TIT and the TOT as close as possible to the design operating conditions, avoiding any damage
- Perform a correct combustion burning all the fuel entering the combustor, maintaining a specific concentration of O_2

For the low-pressure side are:

- Maintain the inlet pressure of pump P5 at 80 bar
- Maintain the inlet pressure of pump P6 at 120 bar
- Control the outlet temperatures of the intercoolers in the compression system
- Maintain the turbine outlet pressure according to its optimal value

We can use as starting point the same variable pairing used by [19] in his previous work and directly do a more focused analysis. The possible variables coupling is the following:

- w_{fuel} : fuel mass flow entering to the combustor. This variable can be used to control the electric power generated by the cycle; to increase or decrease the combustion power, it is necessary to add or reduce the fuel, thus the power will be directly affected by changing this variable.
- w_{P6} : pump P6 mass flow. The objective of this variable in the process is to moderate the outlet temperature of the flue gas entering to the turbine, thus can be used for the control of the turbine outlet temperature. The turbine inlet temperature will be anyway influenced indirectly by the change of this variable.
- $w_{P_{oxy}}$: pump P_{oxy} mass flow. The mass flow of the oxidant stream is fundamental in the combustion process to ensure the complete transformation of natural gas in the combustion, therefore it is possible to use it as control variable for the oxygen mass composition in the flue gas.
- ω_{P5} : pump P5 rotational speed. Differently from pump P6 and pump P_{oxy} that are ideal mass flow controlled pumps, pump P5 can control the pressure after intercooler IC5 modifying its rotational speed.
- ω_{rel} : relative rotational speed of the compression system. Considering the compression system with an ideal prescribed pressure ratio, this variable influences directly the outlet pressure of the system, that corresponds to the inlet pressure of pump P5, for this reason can be chosen as control variable for the inlet pressure of pump P5.
- w_{cpu} : gas mass flow exiting the process. The low-pressure part of the system can be controlled by varying the overall mass of the working fluid contained in the power cycle thus changing the operating pressure of the system. Increasing or decreasing this variable, we can use it to regulate the pressure.

7.1. Dynamic Behavior

In this section the normalized open-loop responses of the reduced system given inlet step variations are examined. Every test is performed by applying a 0.1% step variation to the input variables at time $t=0$ s, starting from steady state conditions. The results for a matter of order are reported all together at the end of the section.

Fuel mass flow step response

The present test is performed by applying a step of 0.1% to the nominal fuel mass flow rate. From the figure 7.1, we can observe that the behavior of the variables in this case is almost the same in both the real and the simplified case. First of all, the electric power increases when the fuel is increased and the response is in both cases similar to a first order system response with a time constant of 20s. For this reason, the turbine outlet temperature reacts to the step with a fast increase and then slowly it decreases. The behavior of the oxygen composition is the same and represents the fact that increasing the amount of fuel, the percentage of oxygen in the mix is suddenly decreased. Regarding the pressures, they have all the same behavior, the turbine outlet pressure is the faster one, the ones related to the pumps are slower, especially in the case of reduced fluids.

Pump P6 mass flow step response

The present test is performed by applying a step of 0.1% of the nominal pump P6 mass flow rate. The direct consequence of this step is a decrease in the turbine outlet temperature, this happens because pump P6 sends more CO₂ in the combustion chamber, that regulate the temperature of the combustion. For the same reason the most affected variable from a magnitude point of view is the oxygen composition that undergoes to a rapid decrease. The turbine outlet pressure and the electrical power increase and the pressures at the inlet of both pumps P5 and P6 decrease due to the fact that there is an overpressure, generating the opposite effect before that point. Looking at the figures in 7.2, the results in the real and reduced case for this step are the same and the reduced fluids behave more or less like the real fluid.

Pump Poxy mass flow step response

The present test is performed by applying a step of 0.1% of the nominal pump Poxy mass flow rate. In this case, applying a step to pump Poxy mass flow rate, the quantity of oxygen is increased and in fact the most influenced variable is the oxygen composition. The other responses are quite similar to the ones already discussed for pump P6. In this case, looking at the figure 7.3, the effect on the oxygen composition is also in this case the main affected variable and the other behaviors are more or less the same.

Pump P5 rotational speed step response

The present test is performed by applying a step of 0.1% in the nominal rotational speed of pump P5. In this case the most affected variable is the inlet pressure of the pump P6.

The order of magnitude of the variation is at least 10 times more than the variation in any other variable. This confirms the idea to use this variable to control the inlet pressure at pump P6. In this case, as can be observed from 7.4, the effect on the inlet pressure of pump P6 is well represented by the reduced fluids and also the others variables behavior is more or less the same.

Compression System relative rotational speed step response

The present test is performed by applying a step of 0.1% of the nominal relative rotational speed of the compression system. The direct effect of this variable is an increase of the pressure at the inlet of pump P5 and consequently at the inlet pressure of pump P6. Looking at the hot side variables, the TOT is decreased and the electrical power is increased. As can be observed in 7.5, the dynamical behavior of the plant with reduced fluid is practically the same of the real one.

Outlet CPU mass flow step response

The present test is performed by applying a step of 0.1% of the nominal CO₂ Procession Unit (CPU) mass flow rate. The step on this variable directly affects all the variables of the low pressure side of the plant (inlet pressure of pump P5 and P6 and the outlet pressure of the turbine). Increasing the outgoing flux of the plant, the system is depressurized and all these variables constantly decrease. On the other side of the plant, this step creates an increase in the electrical power and a decrease in the TOT. From 7.6 can be observed that also in this case, the general dynamic behavior of the variables with respect to the real plant is respected.

7.2. Conclusions

in general, from the analysis of the step responses we can conclude that in the hot side of the plant, there is an important coupling between different pairs of manipulated and controlled variables and the oxygen concentration is highly sensitive to several control inputs. The manipulation of these variables is complicated and will be discussed in the next Chapter. Regarding the low pressure side of the plant, the CPU mass flow rate, the rotational speed of pump P5 and the compression system relative rotational speed are the most influential variables and should be used to control these low pressure side variables. About the results obtained with the reduced fluids, we can say that the behavior of the responses is practically the same to the one obtained with the real mixture, in general very accurate, the main difference is only in the magnitude of some variations. These

little differences are related to the fact that we have simplified the model, neglecting some contributions. This fact does not influence the behavior of the dynamical responses but affects (in some cases) their order of magnitude.

The last thing to underline is that in this case are not reported the responses in the case in which the oxidant flow is simplified with the model with oxygen tracking because the responses are the practically the same apart from the magnitude of a few variables.

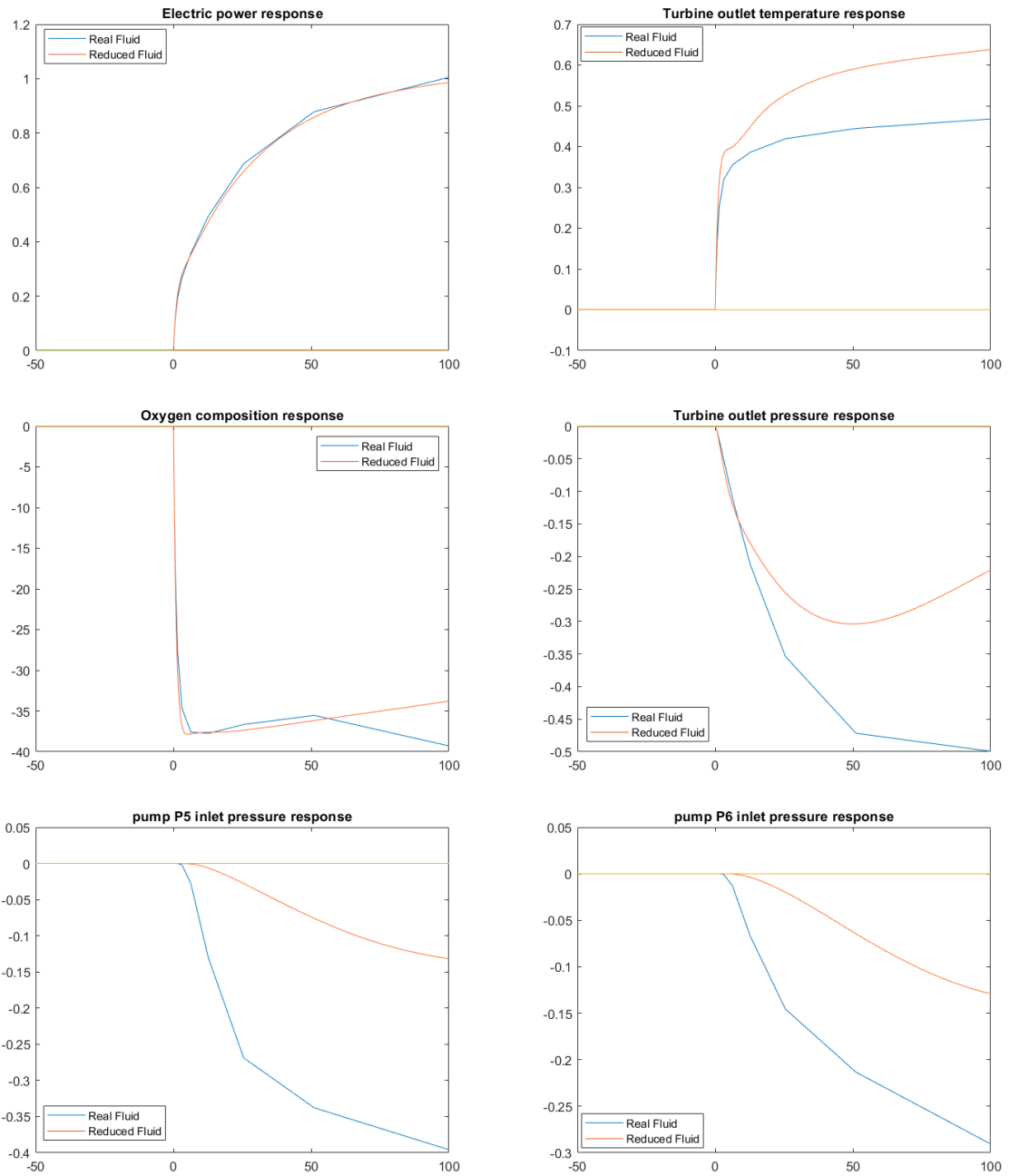


Figure 7.1: Open-loop fuel mass flow rate step responses

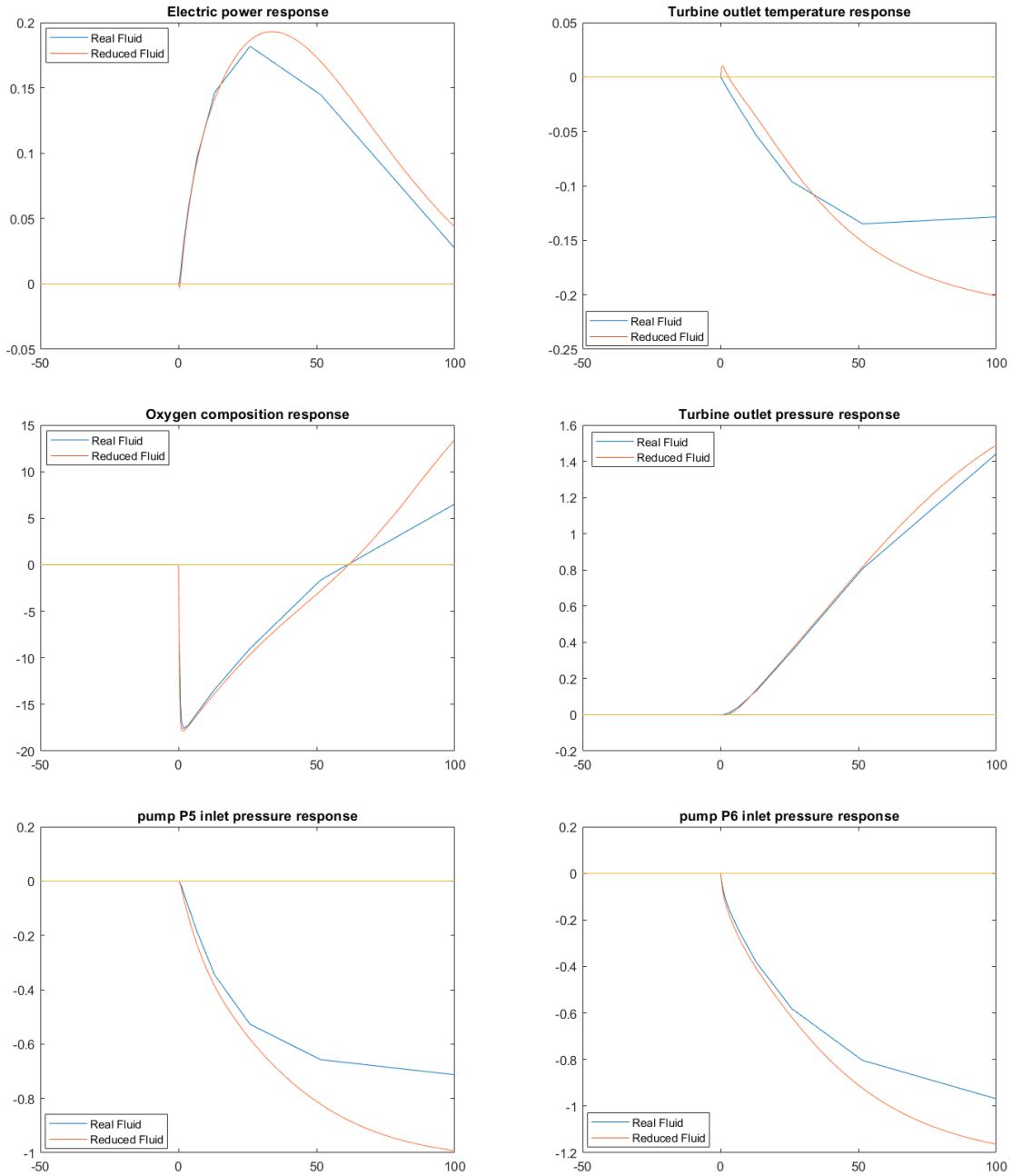


Figure 7.2: Open-loop pump P6 mass flow rate step responses

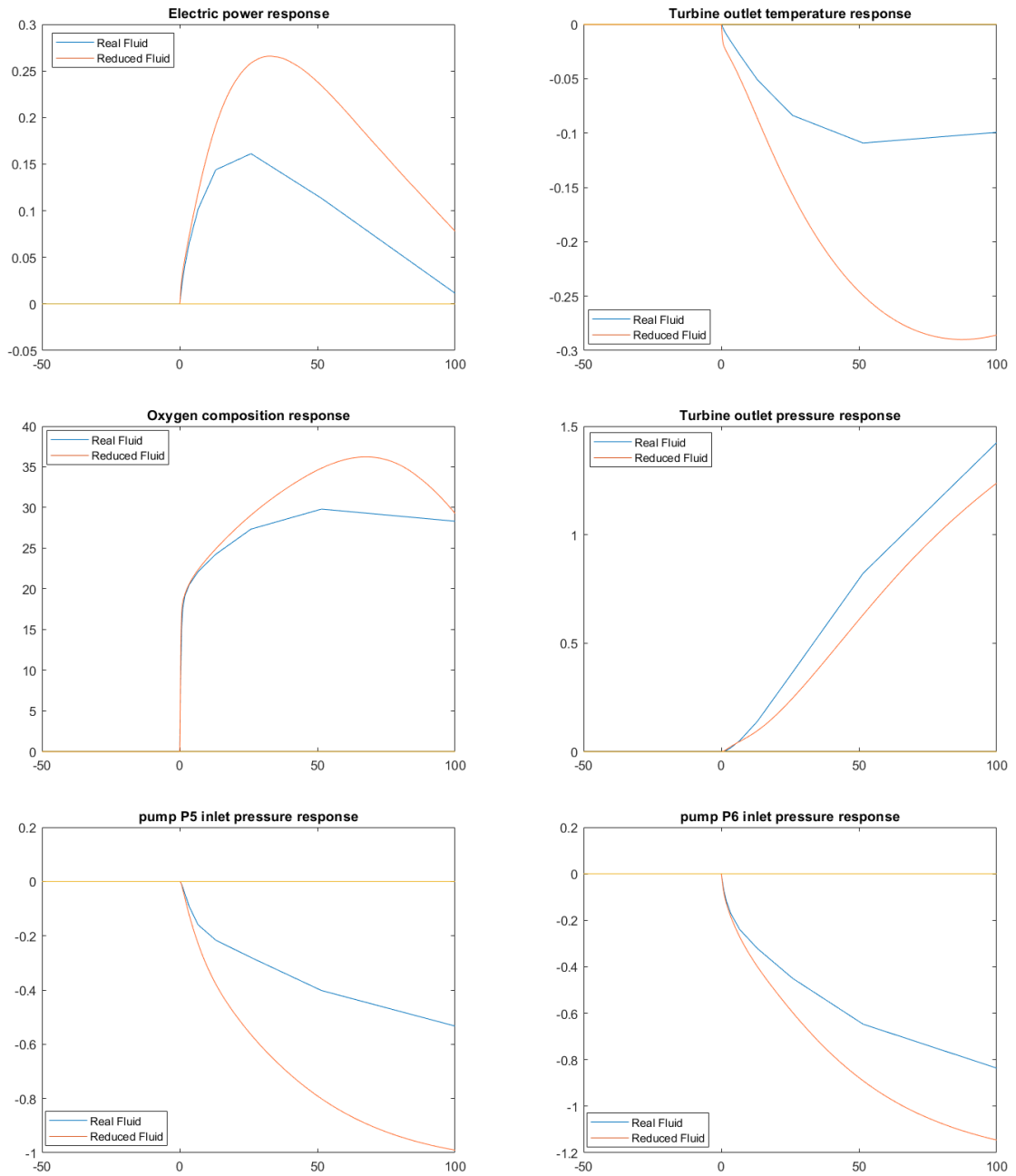


Figure 7.3: Open-loop pump Poxy mass flow rate step responses

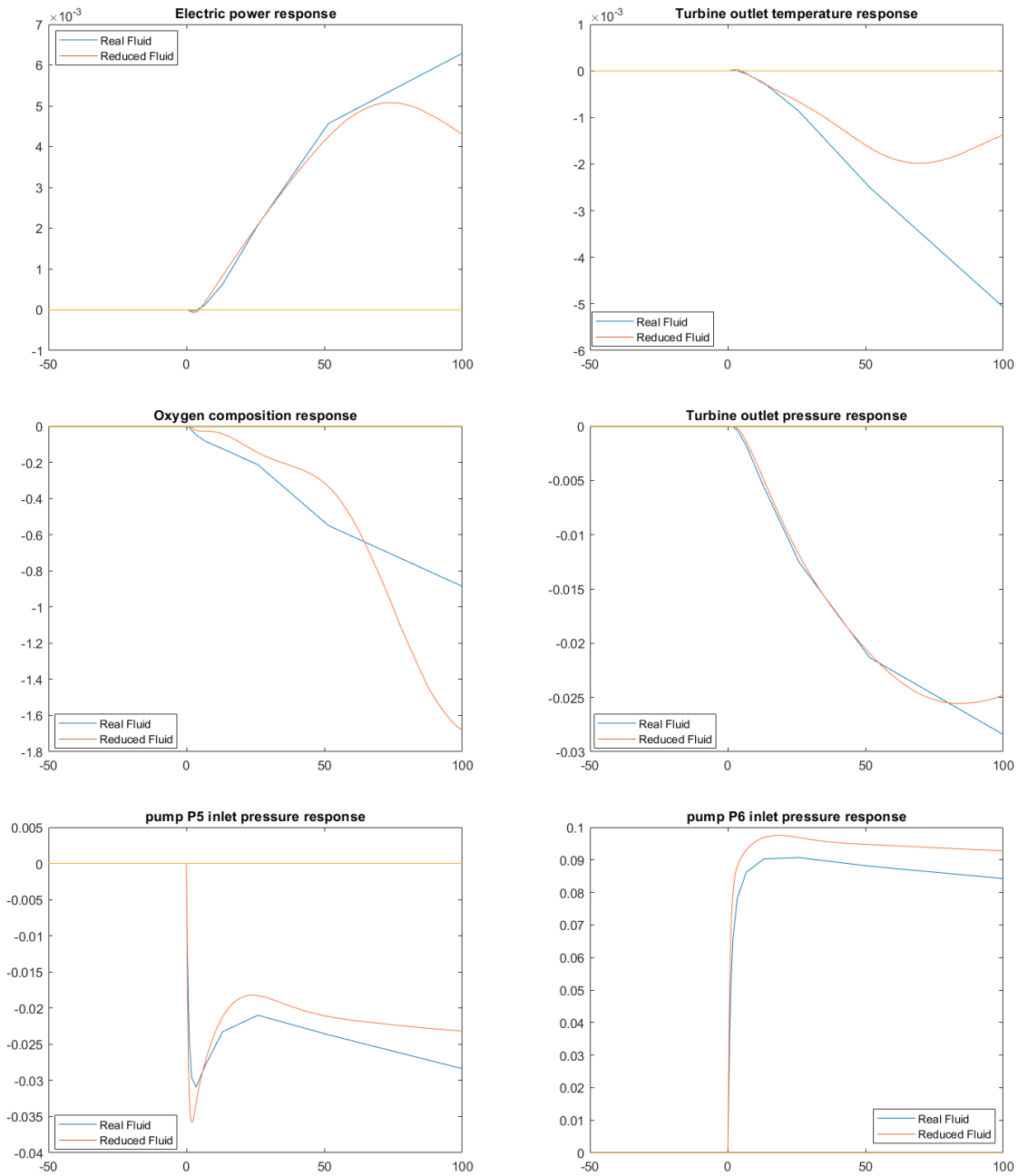


Figure 7.4: Open-loop pump P5 rotational speed step responses

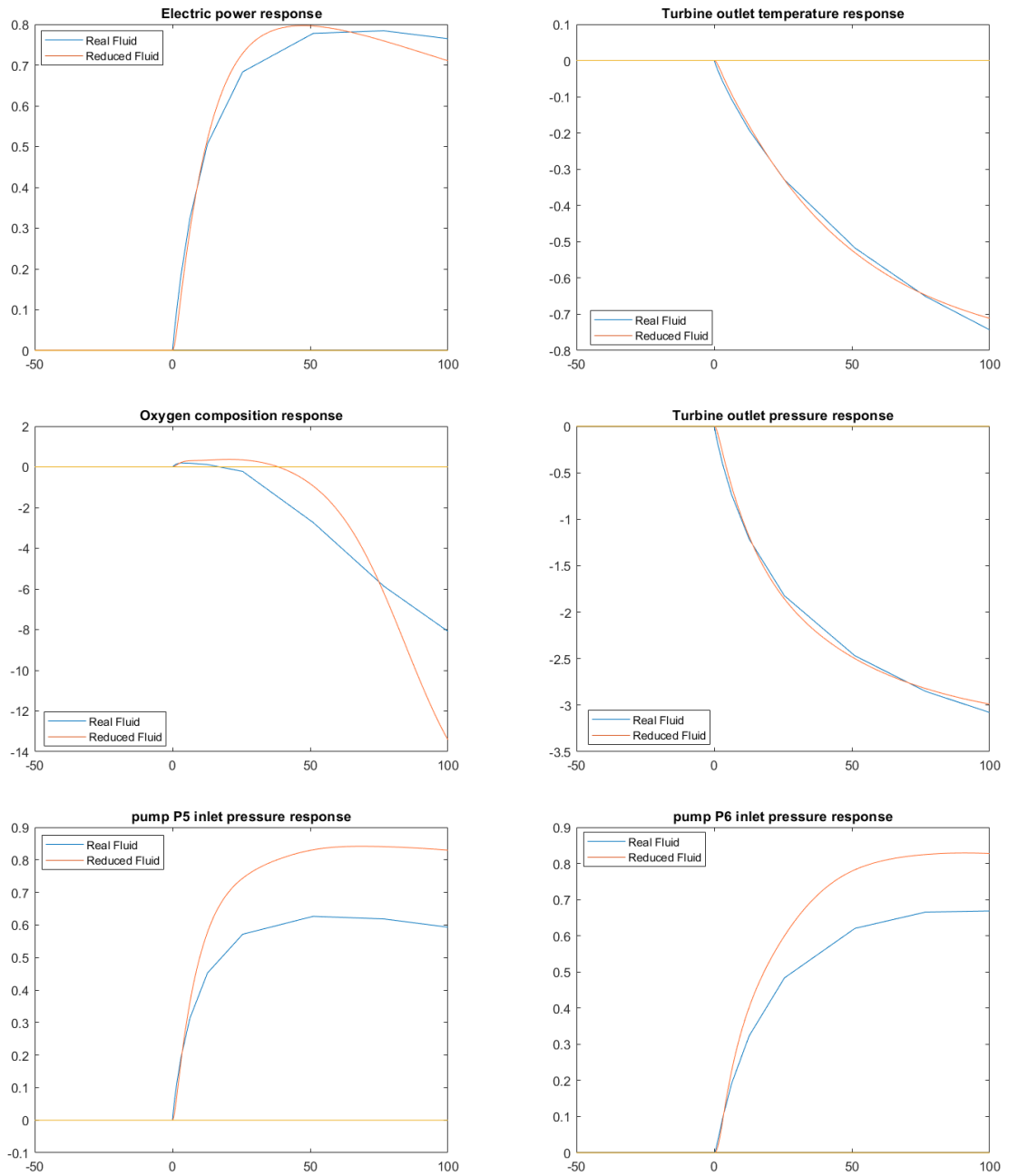


Figure 7.5: Open-loop compression system relative rotational speed step responses

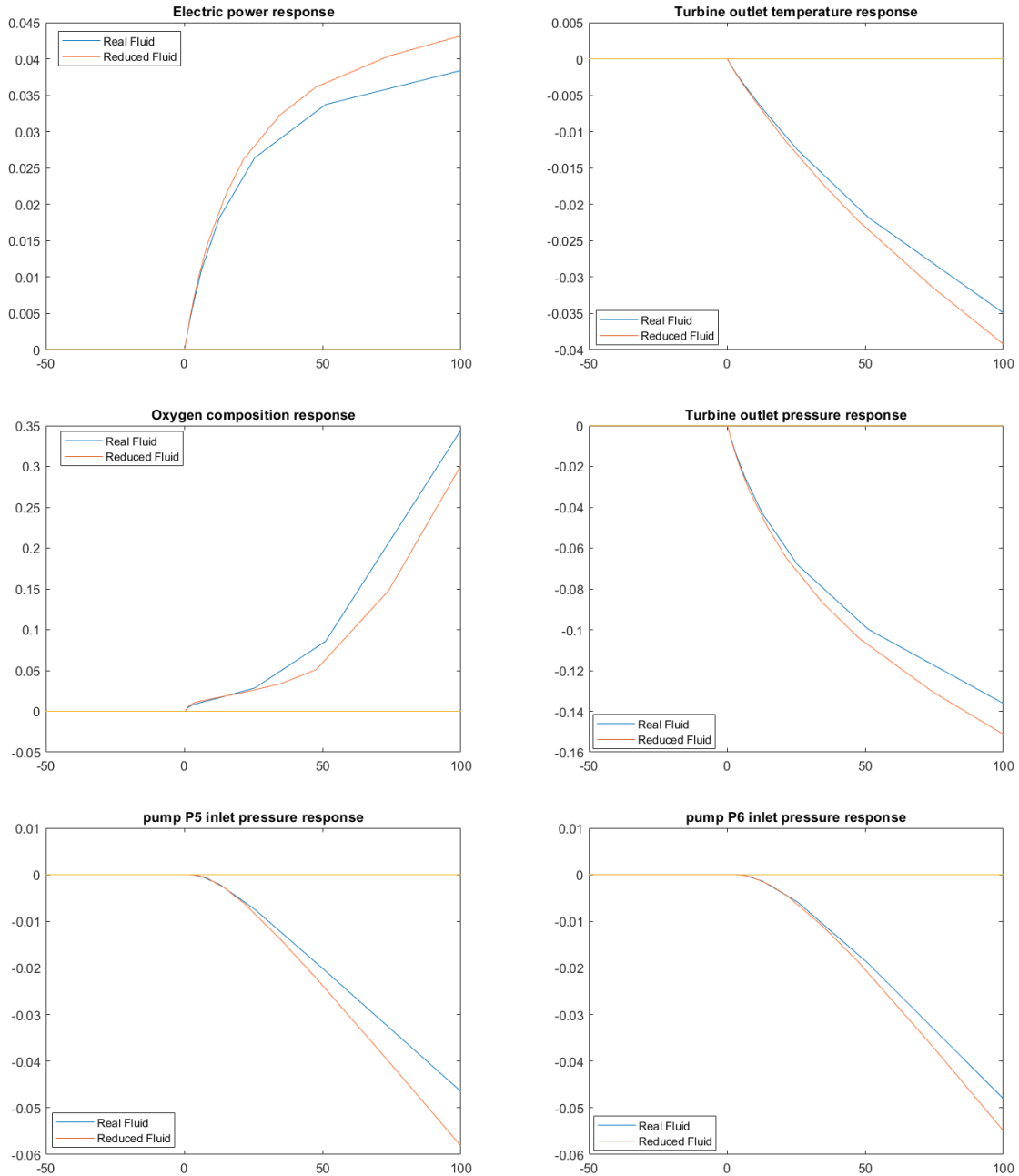


Figure 7.6: Open-loop CPU mass flow rate step responses

8 | Model Based Control Logic

In this last chapter the behavior of the plant with the reduced fluids when a control scheme is applied will be analyzed. In the case of energy plant control, there are some hints to be followed in order to create complete and robust control scheme [8]. It is better to maintain the control scheme as simple as possible and prioritize the control loops required to maintain the various process flows and inventories. From the point of view of stability, feedforward control is better than closed-loop control, if it is possible avoid using closed-loop control, if not, use feedforward control as much as possible, to reduce the effects of disturbances and to guarantee inherent stability. Use the fastest control system and provide high maneuverability for the plant in order to have the possibility to make load changes as fast as possible.

In my work of thesis a new control scheme has not been created, the one described in the next section is the same designed by [19] in its previous work. The aim of the chapter is to verify if the changes and the simplifications done on the fluid model affect the functionality of the control scheme or it is still robust enough to totally control the plant.

8.1. Control Structure

The overall control scheme is composed by low-level controllers and high-level controllers. The aim of the low-level controllers is to obtain faster inner loops that can reject disturbances, simplifying the work of the controllers in the high-level part. The high-level controllers are feedforward and closed loop techniques used to control all the fundamental variables in the plant.

8.1.1. Low-level Control

- **Control of the cooling gas flow**

The objective of this control is to maintain the desired mass flow rate in the cooling stream (CF01-CF02). This stream is the one of the two created by pump P6 that is used to moderate the temperature at the inlet of the turbine (CF02 in Fig. 6.23) to avoid mechanical damages and will be used as manipulated variable in the high

level control of the plant. The aim of the control is to regulate the valve in order to obtain the desired cooling mass flow rate entering in the turbine. We want the controller to be ideally fast, for this reason a component that prescribes the desired mass flow rate is used.

- **Control of the oxidant gas flow**

The objective of this control is to maintain the desired mass flow rate in the oxidant stream (OX02-OX03). This stream is the one coming from pump Pox_y and is used as manipulated variable in the high level control of the plant. As already described in section 6.3, pump Pox_y and P6 are modeled in order to be used to prescribe and ideal mass flow rate. This controller is also assumed to be sufficiently fast to do not create any problem to the rest of the plant.

- **Control of the recycle gas flow**

As before, the objective of the control is to maintain the desired mass flow rate in the recycle stream (RE04-RE05). This stream is the other one of the two created by pump P6 that is used to moderate the combustion temperature inside the combustor. As already described in the previous section, pump P6 can be used to prescribe an ideal mass flow rate, for this reason, given the mass flows prescribed by the cooling control system and the pump P6, the recycle mass flow is the difference between these two controlled streams.

- **Control of oxygen flow**

This control aims to maintain a prescribed mass flow in the oxygen stream coming from the ASU. A specific model of the ASU is not present in the work, for this reason a prescribed mass flow rate source is used. It is important to underline that this stream also prescribes the mass fraction of O_2 of the oxidant stream, that becomes a manipulated variable in the high level controller of the plant.

- **Control of outgoing gas flow to CPU**

This low-level controller has the objective to control the quantity of gas flow outgoing from the cycle to the through the CPU. This variable will be used as manipulated variable in the high-pressure control scheme and since there isn't a specific model for this equipment, this outgoing mass flow is considered as ideally prescribed.

- **Control of the intercooler outlet temperatures**

Finally, the last low-level controller aims to set a fixed temperature at the outlet of each compressor in the compression system. This is needed in order to always work under the best possible conditions and reduce the compression work. This is done by using the simplified ideal model of the intercooler, where the imposed

inlet temperature of the intercooler is used to impose the inlet temperature of the successive compressor (Fig. 8.1).

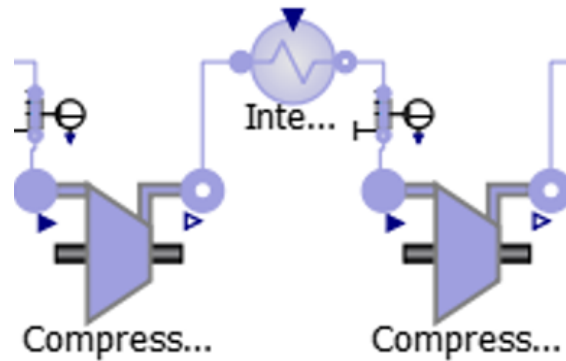


Figure 8.1: Scheme of one intercooler in the compression system

8.1.2. High-level Control

In this section will be discussed the control strategies applied to system in order control the fundamental variables of the system, in particular the electrical power, the TOT and the concentration of oxygen in the hot side of the plant and the inlet pressures of pump P5 and P6 and the turbine outlet temperature for the cold side of the plant. Following the hints given in the introduction of the chapter, in the first section will be analyzed the feedforward actions applied to the system, in the second one will be discussed the static decoupler used in the combustor and the inverse dynamics of the flows and in the last one the controls used for the pressures.

Feedforward control

The feedforward actions applied to the system are the following:

- **Intercooler outlet temperature**

As described in the previous section, the outlet temperature of each intercooler is maintained constant by the intercooler, a feedforward action is used to keep this value constant also at low level conditions.

- **Cooling mass flow rate**

As already underlined in section 6.5, the turbine model used in the plant is a reduced model of the specific turbine designed for the cycle. For this reason there are no principles to correctly set the correct cooling flow. The feedforward action used to increase or decrease the mass flow directly depends on the thermal load.

Static decoupler and Inverse dynamics

In this section the techniques used to manipulate the variables in the hot side of the plant will be discussed. This necessity arises from the fact that from the step response analysis carried out in the previous chapter, there is a strong coupling between these variables that increase the difficulty in the control system design.

The final variables that need to be controlled are the flue gas mass flow w_{flue} , the outlet temperature of the combustor T_{flue} and the oxygen composition at the outlet of the combustor X_{O_2} . The manipulated variables are the mass flows prescribed by pumps P6 and Poxy and by the fuel supply system. Obviously, between the manipulated variables there is some dynamics that could be difficult to be managed during the controller design. The scope of this step is to obtain the approximated relationship between these variables in order to get the required manipulated variables (w_{P6} , w_{Poxy} , w_{fuel}) based on the desired ones (w_{flue} , T_{flue} , X_{O_2}).

Due to the composition of the plant, this procedure can be divided into two different steps: the first one in which the input variables of the combustor w_{oxy} , w_{re} and w_{fuel} (intermediate set point variables), are expressed by our objective variables (static decoupling), and the second one in which the actual manipulated variables, the prescribed pumps mass flow rates, are expressed by the intermediate setpoints, the combustor input flows (inverse dynamics). In this way we could be able to express the manipulated variables depending on the desired values of the controlled variables.

Looking at the figure in 6.22 it is straightforward to understand that the flue gas properties (temperature, mass flow rate and oxygen composition) basically depends on the input streams and the chemical reactions that occur inside the combustor. The scope of the static decoupler is to look for a static relation between these variables. To do so we can use the mass balance equation (8.1), the gas energy balance equation (8.2) and the oxygen mass balance equation (8.3) to obtain the values of the three input flow rates as a function of the desired values of oxygen concentration and flue gas mass flow and temperature.

$$0 = w_{fuel} + w_{re} + w_{oxy} - w_{flue} \quad (8.1)$$

$$0 = w_{fuel} \cdot h_{fuel} + w_{re} \cdot h_{re} + w_{oxy} \cdot h_{oxy} - w_{flue} \cdot h_{flue} \quad (8.2)$$

$$0 = w_{re} \cdot X_{O_2,re} + w_{oxy} \cdot X_{O_2,oxy} - w_{flue} \cdot X_{O_2,flue} - 2w_{comb} \cdot MM_{O_2} \quad (8.3)$$

Once obtained the values of the combustor input flows as a function of the controlled variables, we have now to obtain the relationships between these intermediate set point variables and the actual manipulated variables that are the mass flow rates of pumps P6 and Poxy and compute the inverse dynamics. Recalling the theory from [10], the idea is to create an electrical equivalent of this part of the system between the pumping system and the turbine and evaluate the dynamics (transfer function) between the variables analyzing this equivalent circuit. In particular from the theory and writing down the mass and momentum balance equations for a pipe with a compressible fluid, we can approximate its behavior as the one of a capacitance obtaining:

$$\Delta w_{in} - \Delta w_{out} = C \cdot \frac{d\Delta p}{dt} \quad (8.4)$$

$$C = \frac{M}{p} \quad (8.5)$$

The same approach, under the hypothesis of choked flow and compressible fluid can be applied to the turbine, obtaining that the behavior of a turbine can be approximated as resistance with the value in 8.6.

$$R = \frac{p_{in}}{w} \quad (8.6)$$

From the previous considerations we can represent the pumps as current generators that prescribe the current, the streams of the regenerator as long pipes and the resistance of the combustor can be neglected compared to the dominant one of the turbine.

This analysis brought us to the conclusion that this part of the plant can be approximated as an RC circuit (Fig. 8.2) with two ideal prescribed flow sources given by the pumps, two capacitors given by the pipes and one resistor that represents the turbine.

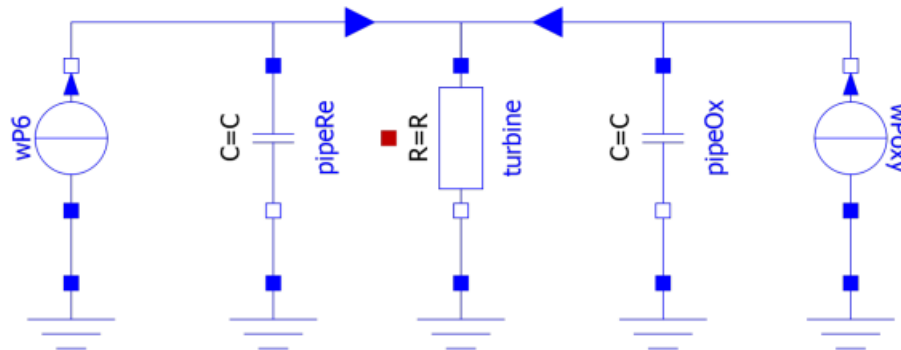


Figure 8.2: Electrical equivalent circuit of the hot side of the plant

From the electrical scheme we can estimate the transfer functions of the system:

$$\frac{w_{oxy}(s)}{w_{P_{oxy}}(s)} = \frac{1}{\tau s + 1} \quad (8.7)$$

$$\frac{w_{re}(s)}{w_{P_{oxy}}(s)} = \frac{-\tau s}{\tau s + 1} \quad (8.8)$$

$$\frac{w_{oxy}(s)}{w_{P_6}(s)} = \frac{-\tau s}{\tau s + 1} \quad (8.9)$$

$$\frac{w_{re}(s)}{w_{P_6}(s)} = \frac{1}{\tau s + 1} \quad (8.10)$$

With this circuit it is possible to estimate the residence time of the system τ_r which is twice the time constant of the system. In this case $\tau = \frac{RC}{2}$ and using the formulas in 8.5 and 8.6 it is possible to calculate the numerical values. Considering that the mass is around the $91.5 \cdot 10^3 Kg$ and the mass flow rate is equal to 1308.88 kg/s, the time constant of the system and the residence time are respectively $\tau = 35s$ and $\tau_r = 70s$. It is important to notice that the time constant is practically invariant with the load, at half load the temperatures are more or less the same, the turbine flow is reduced by a half and the same for the pressure, obtaining an invariant time constant.

Finally, the inverse dynamics of the fuel mass flow is simpler since it is assumed that its behaviour is similar to a first order system. It is possible to compute the inverse dynamics and add a low-pass filter into the system. The oxygen concentration in the flue gas is not taken into account in this manipulation because as in the case of the fuel mass flow rate, its dynamics is simpler.

Applying this approach, we obtained the decoupling of these variables, simplifying the highly non linear system into one more manageable, simplifying also the controller design. At this point, to control the hot side of the plant, due to the fact that each loop corresponds to a first order system, it is possible to use simple PI controllers.

Pressure control

Using the procedure described here above we have been able to control the hot side of the plant, it is now necessary to control also the cold side of the plant, i.e. the inlet pressures of the of pumps P5 (pinP5) and P6 (pinP6) and the turbine outlet pressure (TOP).

From the step response analysis we decided to control these three variables respectively with the relative rotational speed of the compression system (ω_{rel}), the rotational speed of pump P5 (ω_{P5}) and the outgoing mass flow rate of the CPU (w_{CPU}). As already said,

even if the step response analysis gave us this results, it is important to verify if there exist a coupling between these specific variables. In order to do so, the system (with closed loops for the hot side variables), have been linearized using the numerical method embedded in Dymola and then an RGA analysis have been done in order to verify the coupling of these variables. From the matrix in 8.11, it is possible to see that the diagonal values are all close to one and all the others close to zero. It is now possible to conclude that we are able to control these variables independently using the selected manipulated variables.

$$RGA = \begin{bmatrix} 0.965 & 0.100 & -0.065 \\ 0.103 & 0.900 & -0.003 \\ -0.068 & 0.006 & 1.068 \end{bmatrix} \quad (8.11)$$

At this point, to independently control these variables it is possible to design three PI controllers, choosing the best value for the cross-over frequencies.

This section also conclude the description of the control techniques applied to the cycle when reduced fluid are used. As already mentioned in the introduction to this chapter, the controllers applied to the system are the same already designed in its previous work by Muro Alvarado [19]. Summing up, the overall control is based on the feedforward actions, the low-level control and the high-level control, composed by two control logics (inverse dynamics and static decoupling) and six independently designed PI controllers.

8.2. Results

In this last section will be analysed the behavior of the control scheme and of the plant in a realistic scenario. In this case, we will consider a situation where the system goes from 100% to 30% of the thermal load and back in 7×10^4 seconds. From this test we want to analyse both the static and dynamic behaviors of the system and of the controllers at different thermal loads.

Another thing that we want to verify is that the plant with the reduced fluids can be controlled and behaves as the real plant at different thermal loads. The applied fluids are the ones already described in chapter 6. The last thing to underline is that until now, by using the oxygen tracking model (6.1.5) or the CO₂ + oxygen model (6.1.4) for the oxidant stream, the same results have been obtained, but when the controllers are applied to the system the situation changes. The results that will be discussed here below are referred to the model composed by CO₂ and oxygen because when the oxygen tracking model is used coupled with the controllers, it creates an unstable behavior of the variables, nullifying the action of the controllers and crashing the simulations. This result can be explained

by the fact that this is the only fluid model that is built differently from the others. The pure CO_2 , $\text{CO}_2 + \text{water}$ and $\text{CO}_2 + \text{oxygen}$ models are built in the same way of the real mixture, only removing some species from the mix. On the other side, the oxygen tracking model is basically a pure CO_2 model with some software and model corrections in order to measure and track the quantity of the oxygen in specific parts of the system. This differences could have created some differences in the final model and during the simulations this could have brought to wrong and divergent solutions computed by the solver.

8.2.1. Static Analysis

In this section will be discussed the static results given by the control scheme under the thermal load setpoint described in the introduction to the section. Looking at the table in 8.1, the error between the real and the simplified plant at nominal conditions and at 30% of the load is very low, abundantly under the 0.1%. This behavior could be expected since the electrical power is the controlled variable. The error due to the model simplifications is reflected by the fuel mass flow rate that need to be increased or decreased to reach the prescribed electrical power. In the same table, the results regarding the fuel mass flow rate are reported and the error is around the 1.3% in the worst case, still acceptable for our purposes. The first conclusion that can be made is the fact that even with reduced fluids, the control scheme is robust enough to keep under control the variables of the plant, or in another way, the simplified model is not so wrong with respect to the real one to be uncontrollable by the same control scheme.

Other important variables to be evaluated are the ones connected to the turbine. In table 8.2, can be observed the values of the turbine inlet temperature and turbine outlet pressure and also in this case the results are practically the same of the real plant and the error is below the 0.01%. These two variables have been taken into consideration because are two of the objective variables controlled by our control scheme.

Load %	Real Mixture		Reduced Fluid		Error %	
	P_{net} MW	w_{fuel} Kg/s	P_{net} MW	w_{fuel} Kg/s	ΔP_{net} %	Δw_{fuel} %
100	500.06	16.52	499.89	16.40	0.04	-0.73
30	124.96	4.82	124.96	4.88	<0.01	1.24

Table 8.1: Plant net power and fuel mass flow rate controlled static response

Turbine Load %	Real Mixture		Reduced Fluid		Error %	
	P_{out} bar	T_{in} °C	P_{out} bar	T_{in} °C	ΔP_{out} %	ΔT_{in} %
100	30.60	1144.39	30.60	1144.39	<0.01	<0.01
30	18.00	1050.45	18.00	1050.45	<0.01	<0.01

Table 8.2: Turbine inlet temperature and turbine outlet pressure controlled static response

The final important parameters to be evaluated are the temperatures of the streams at the outlet of the regenerator. From the results in 8.3, it is possible to see that the results are acceptable, they respect the ones obtained in the previous steady-state analysis. In conclusion, the static analysis confirms that the control logic is able to control the plant also in the case in which reduced fluids are applied.

Regenerator 100% load	Real Mixture	Reduced Fluid	Error %
	T_{out} °C	T_{out} °C	ΔT_{out} %
Oxidant	707.59	706.44	-0.16
Moderator	707.39	706.15	-0.17
Cooling	150.67	141.45	-6.12
Flue Gas	66.27	56.26	-15.10

Regenerator 30% load	Real Mixture	Reduced Fluid	Error %
	T_{out} °C	T_{out} °C	ΔT_{out} %
Oxidant	688.58	674.39	-2.06
Moderator	689.16	685.35	-0.55
Cooling	30.72	25.91	-15.65
Flue Gas	23.24	20.20	-13.08

Table 8.3: Regenerator outlet temperature controlled static response

8.2.2. Dynamic Analysis

Last thing to do is to analyse the dynamic response of the system under the scenario in which the load varies from the 100% to the 30% in 12.5 minutes, that is equal to a variation of the 5.6% per minute.

The most important variable is the net power produced by the plant. As can be observed in figures 8.3 and 8.4, the plant is perfectly able to track the setpoint without any relevant fluctuation. The difference between the responses in the real and reduced case are practically negligible.

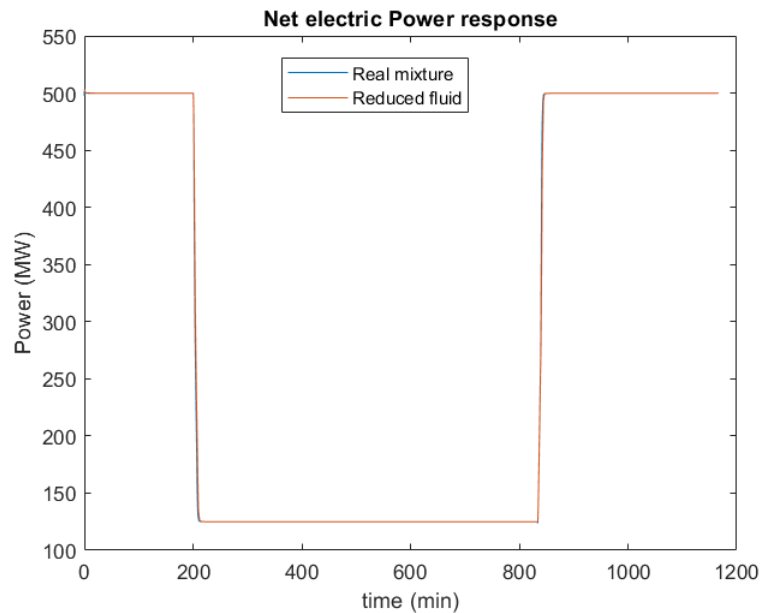


Figure 8.3: Net power dynamic response

Fig. 8.5 and 8.6 represent the dynamic response of the TOT, its nominal value should be around 725°C but as can be observed, during the variation of the thermal load (at the ramps) there are some fluctuations. In the case of reduced fluids these fluctuations are smaller in order of magnitude but the behavior is the same obtained with the real mixture, the maximum error is around the 0.5%, which is an acceptable error. On the other hand, the inlet temperature of the turbine (Fig. 8.7 and 8.8), that is not a directly controlled variable in our scheme, decrease and increase with a rate of 8°C per minute. The response is not perfect as the one of the net power but the tracking is still very good and the same observations made for TOT can be done.

Regarding the inlet pressures of pump P5 and P6 (Fig. 8.9 - 8.10 and 8.11), the set-points are tracked very quickly, the error in the variation of the pressure in the case of

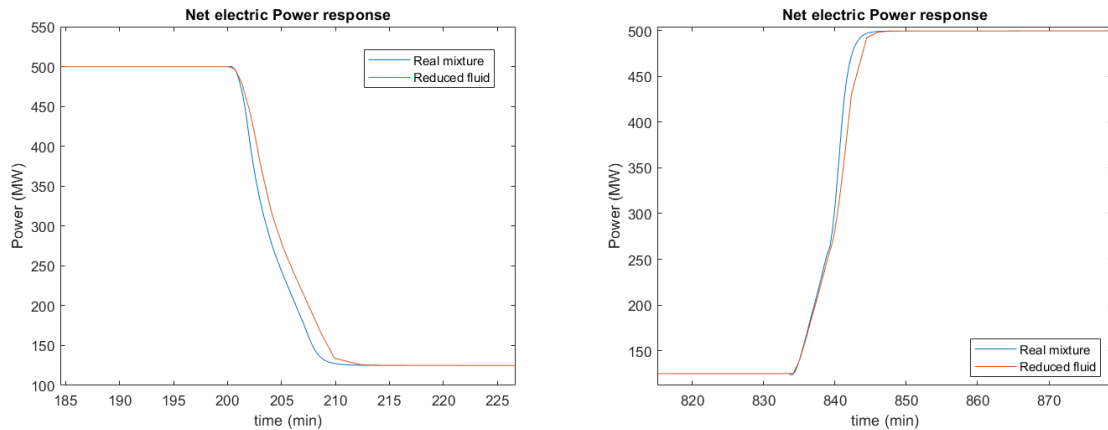


Figure 8.4: Net power dynamic response transients

reduced fluid of pump P5 is a bit less than the error in the case of the real mixture, that is in the worst case lower than the 0.5%. For pump P6 the result is practically the same in both cases with a perfect tracking of the setpoint. The dynamical behavior of the response with the reduced fluids results also in this case a bit more damped than the behavior obtained with the complete mixture.

In figure 8.12 can be observed the evolution of the turbine outlet pressure during the transient and we can say that also in this case the control scheme is able to track the setpoint. The differences between reduced and real fluid are practically negligible. It is important to underline the behavior of the CPU mass flow rate (Fig. 8.13 and 8.14) that is the variable used to control the turbine outlet pressure. As usual from the previous considerations, the fluctuations in the real case are a bit bigger than the ones of the reduced fluid. Even these fact, the overall result can be considered satisfying.

Finally, in figure 8.15 can be evaluated the responses of the three pumps mass flow rates, which are the control actions in our system. Also in this case the responses are practically the same with only in some cases a little error in the steady-state part.

It is now possible to conclude that even with reduced fluids, the control scheme is robust enough to keep under control the variables of the plant, also under huge setpoint variations as the one here presented. On the other side the simplified model is precise and reliable enough with respect to the real one to be controlled by the same control scheme.

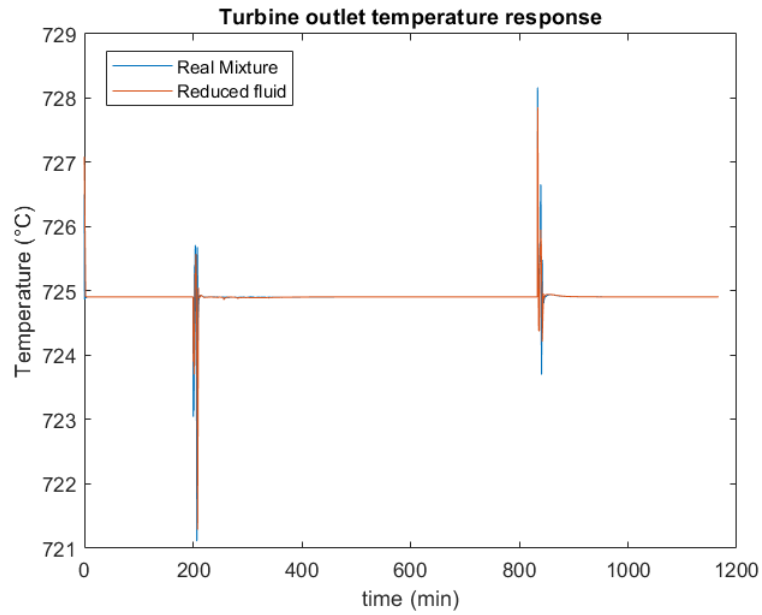


Figure 8.5: Turbine outlet temperature dynamic response

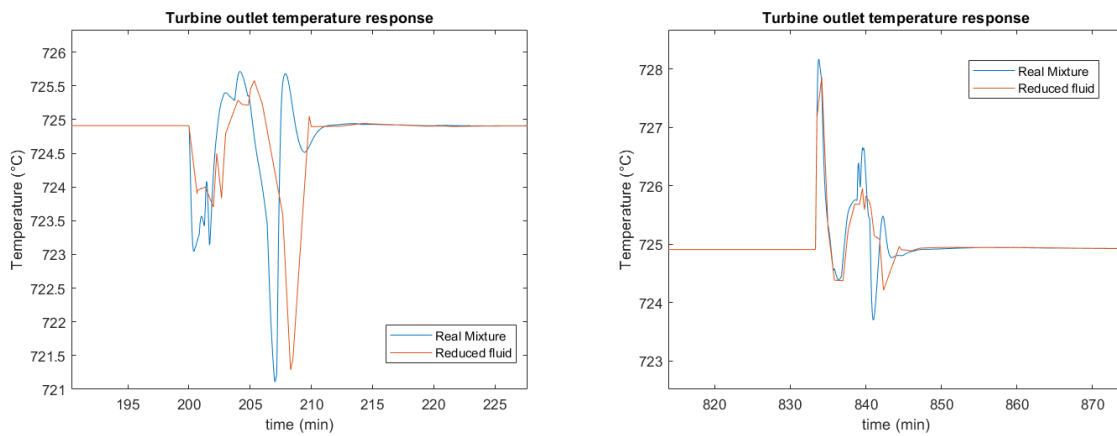


Figure 8.6: Turbine outlet temperature dynamic response transients

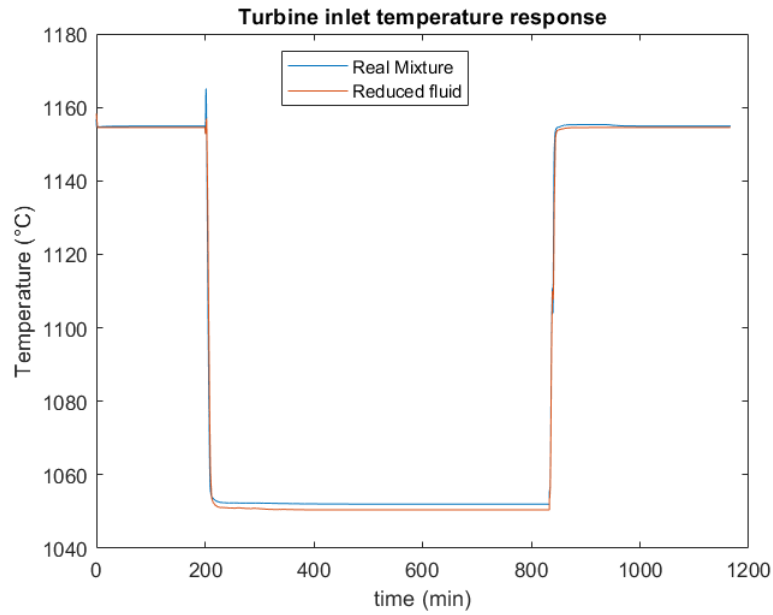


Figure 8.7: Turbine inlet temperature dynamic response

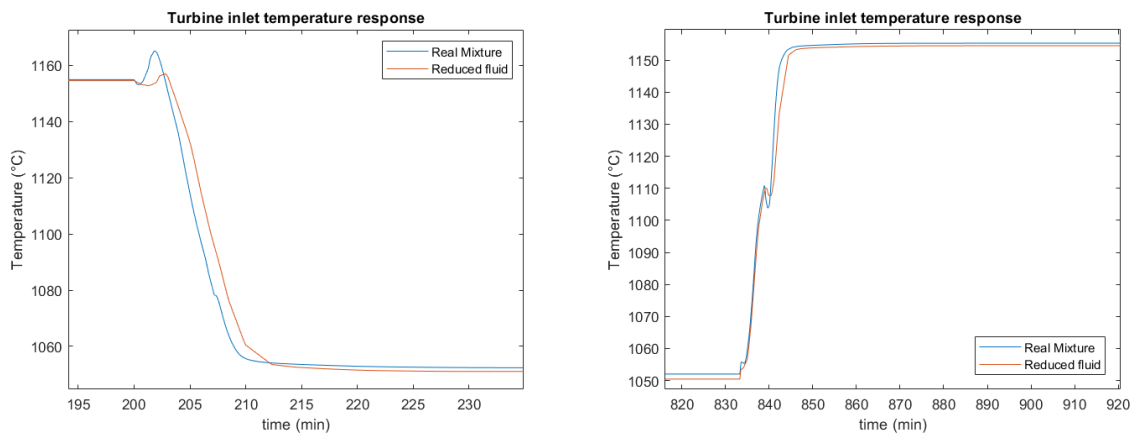


Figure 8.8: Turbine inlet temperature dynamic response transients

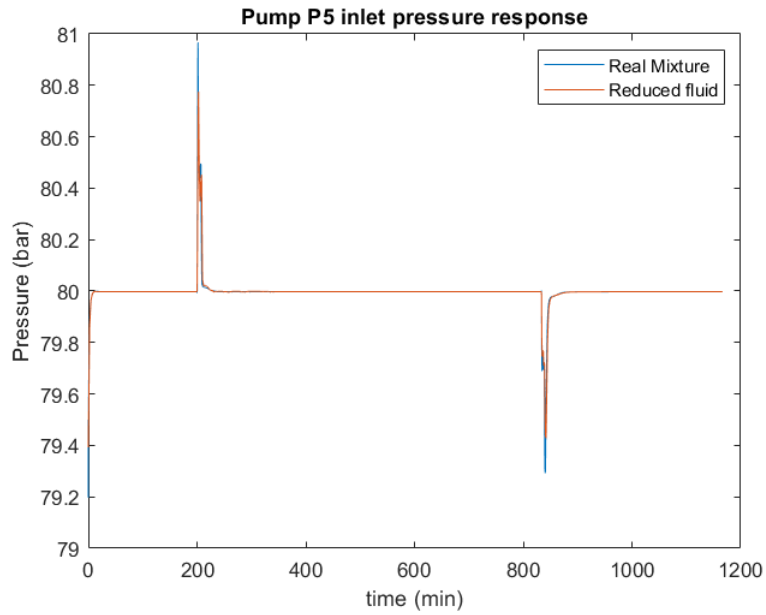


Figure 8.9: Pump P5 inlet pressure dynamic response

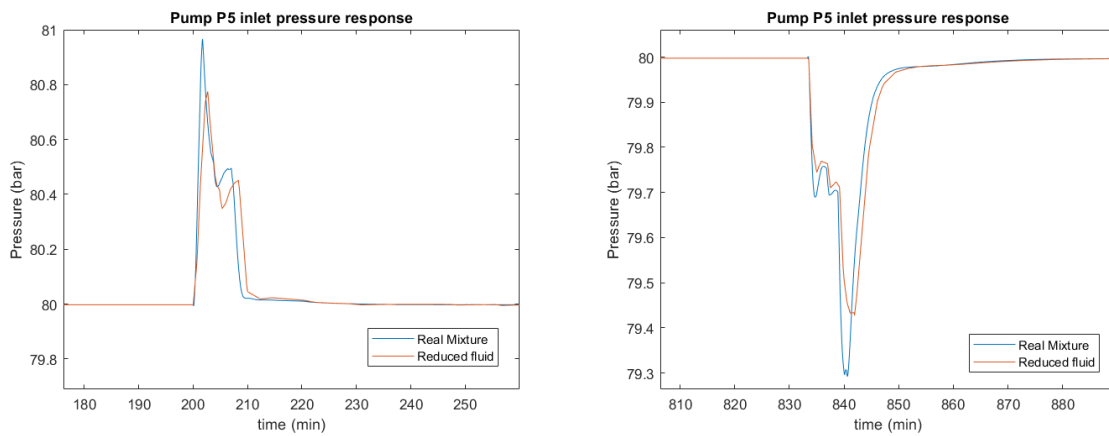


Figure 8.10: Pump P5 inlet pressure dynamic response transients

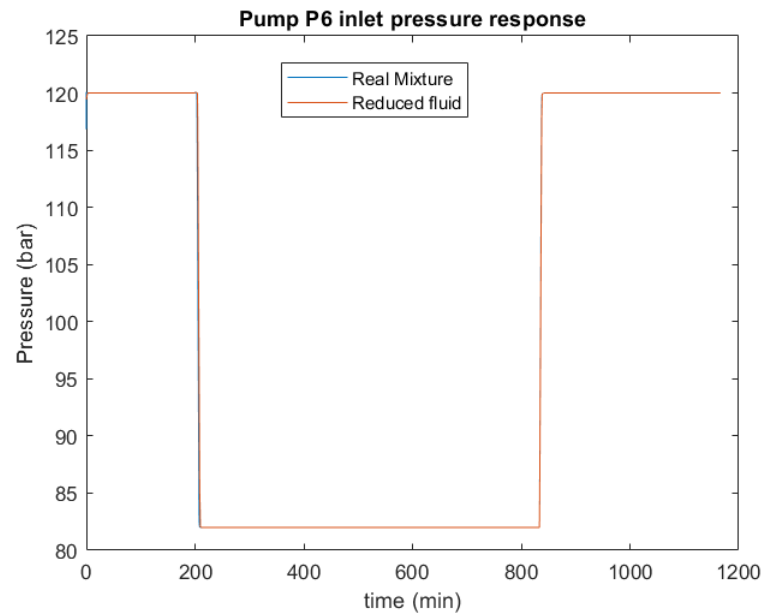


Figure 8.11: Pump P6 inlet pressure dynamic response

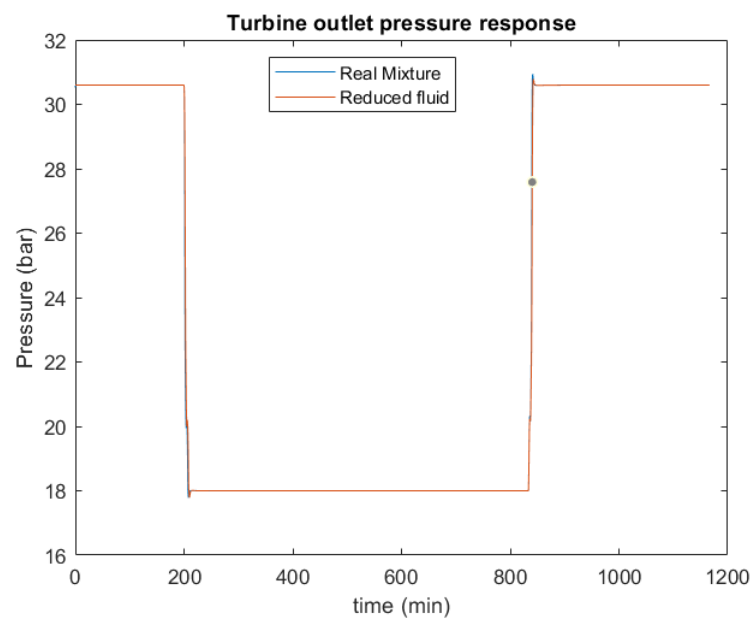


Figure 8.12: Turbine outlet pressure response

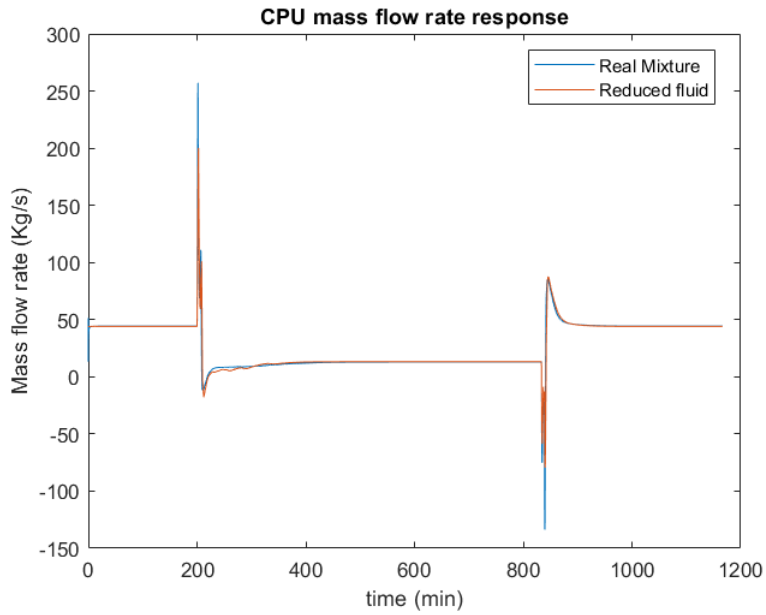


Figure 8.13: CPU mass flow rate dynamic response

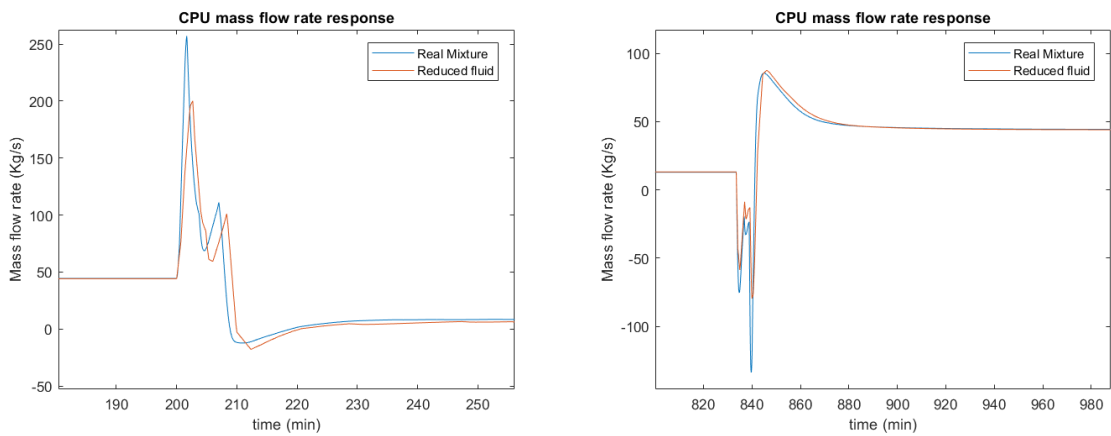


Figure 8.14: CPU mass flow rate dynamic response transients

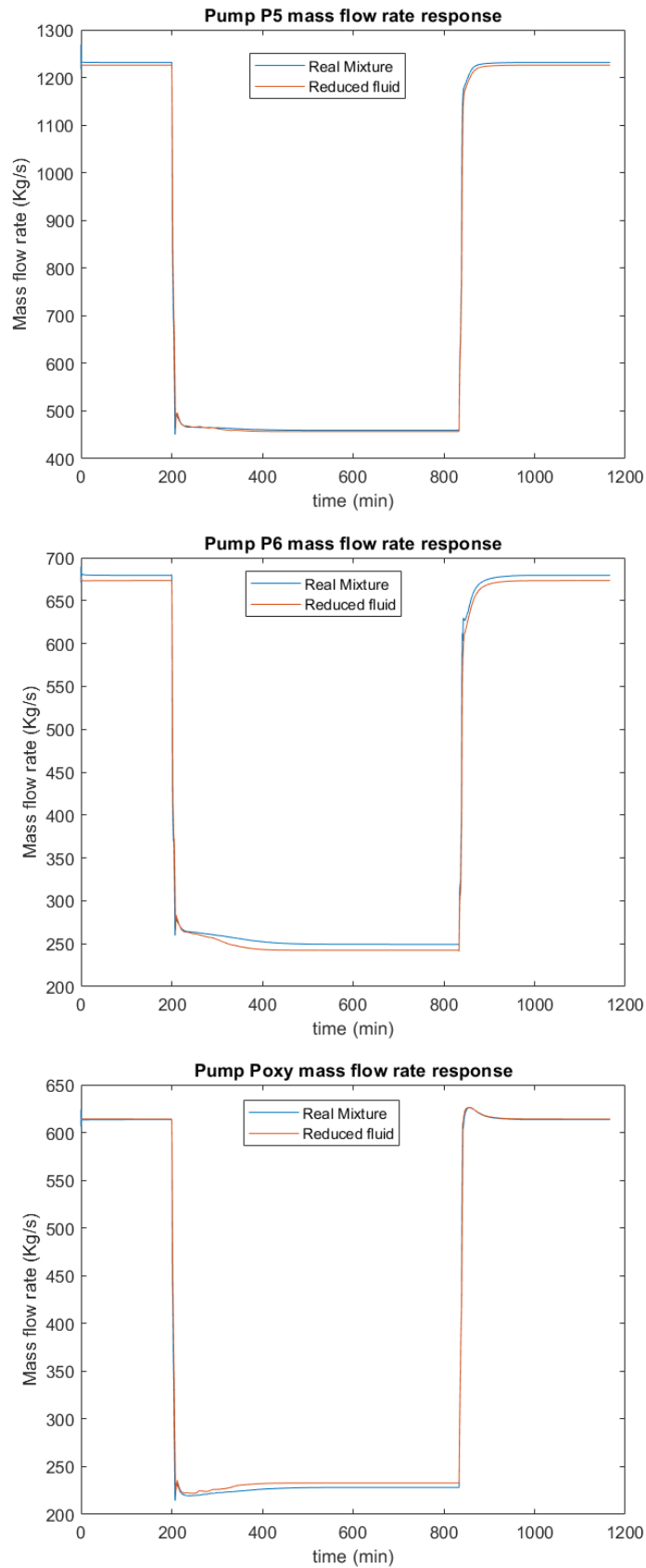


Figure 8.15: pumps P5-P6-Poxy mass flow rate dynamic responses

9 | Conclusions and Future Developments

This study has presented an analysis of the static and dynamic performances of the Allam cycle in the case the real model of the working fluid is simplified in order to obtain a more manageable overall plant model.

Starting from the reduced fluid models, they have been developed in order to reduce the complexity of the actual fluid but still representing the fundamental contributions given by the most relevant components in the real mixture. In particular, three fluid models have been developed, applied in different parts of the plant, relying on the working conditions and phenomena of each zone. For the choice of the simplifications, we had to trade off between the accuracy needed to represent the system and the computational weight of the plant model. The results presented in section 6.1 represents the analysis carried out on the behavior of the three different models with respect to the real mixture.

Next step was to analyze the steady state behavior of each component present in the system and then of the complete closed cycle when the real fluid is replaced with the simplified one. For each component a simple test at nominal conditions was done in order to verify its correctness with respect to the real behavior and then all these components were connected together in order to create the closed cycle and test it at steady state conditions to verify its overall behavior and reliability. Concluding, from the static point of view we obtained good results and we can state that the reduced models are able, at least at the steady state, to represent the behavior of the real mixture.

Once the static analysis was finished, we moved on to analyze the dynamic behavior of the system. In order to do so, for each input variable, we created step responses test, and we observed which are the most affected variables by the specified input. From this analysis we can say that there exist a strong coupling between all the variables related to the hot side of the plant while the cold side variables of the plant are more independent. Looking at the responses of the plant with the reduced fluids, we can observe that, except for the magnitude of some response, the behaviors in the real and reduced case are practically

the same. The dynamic behavior is minimally affected by the simplifications applied to the fluid model but despite that, most of the responses are the same of the real plant and the reduced models are still able to represent the system.

Finally, it is now necessary to verify if the control scheme applied to the real plant is still effective also on the reduced plant. From the excellent obtained results we can conclude that the control scheme is able to perfectly control the variables of the reduced model and the error introduced by the simplifications is not so relevant to lead to an uncontrollable behavior.

Last thing to underline is the fact that the control test is based on two variations of the thermal load from the 100% to the 30% and vice versa in 12.5 minutes each. The good response of the control to these two ramps also confirm the flexibility of the reduced plant to work at different part loads.

In conclusion we have obtained a reduced model with more or less a third of the starting equations and a lot less computationally demanding, so much that it can be fully simulated on standard devices. This without loss of fundamentals static or dynamic information or performances from the control scheme.

Future Developments

The starting model was highly non linear, difficult to be managed and demanding from the computational point of view. Thanks to this work we have been able to reduce its complexity, obtaining a more compact model. This development could also easily bring to new advanced control techniques or other improvements. Some future developments could be the following:

- Create more accurate and specific fluid models able to better represent both the static and dynamic behavior of the system, without increasing the lower complexity obtained through this study.
- Given the flexibility of the model could be useful to apply controllers based on the *gain scheduling*, different controllers at different thermal loads in order to enhance the overall precision of the control scheme.
- Thanks to a more manageable model could be interesting to apply advanced control techniques, such as Model Predictive Control (MPC) (linear or non linear) or Linear Quadratic Control (LQC), and evaluate these results with respect to the actual control system based on PID controllers.

Bibliography

- [1] Dymola Dassault Systèmes. URL <https://www.3ds.com/it/prodotti-e-servizi/catia/prodotti/dymola/>.
- [2] Eurostat - Complete energy balances. URL https://ec.europa.eu/eurostat/databrowser/view/nrg_bal_c/default/table?lang=en.
- [3] Modelica Association. URL <https://modelica.org/>.
- [4] TERNA Driving Energy - Actual generation. URL <https://www.terna.it/it/sistema-elettrico/transparency-report/actual-generation>.
- [5] R. Allam, M. Palmer, and W. Brown. High efficiency and low cost of electricity generation from fossil fuels while eliminating atmospheric emissions, including carbon dioxide. pages 1135–1149. *Energy Procedia*, 2013.
- [6] R. Allam, S. Martin, and B. Forrest. Demonstration of the Allam cycle: An update on the development status of a high efficiency supercritical carbon dioxide power process employing full carbon capture. *Energy Procedia*, 2017.
- [7] F. Allegri. Optimal control of s-CO₂ systems using object-oriented models and tools. Master’s thesis, Politecnico di Milano, 2017.
- [8] P. S. Buckley. *Techniques of Process Control*. Wiley, 1965.
- [9] L. Cabeza, A. Gracia, and M. Farid. Supercritical CO₂ as heat transfer fluid, a review. *Applied Thermal Engineering*, pages 799–810, 2017.
- [10] F. Casella. Advanced process control - [lecture notes]. *Politecnico di Milano*, 2020.
- [11] F. Casella. A Modelica library fo thermal power generation sysyem modelling, October 2022 (last update). URL <https://github.com/casella/ThermoPower>.
- [12] F. Casella and A. Leva. Modelica open library for power plant simulation: Design and experimental validation. *Proc. 3rd Modelica Conference*, 2003.
- [13] V. Dostal, M. Drscoll, and P. Hejzlar. A supercritical carbon dioxide cycle for next

- generation nuclear reactors. *The MIT Center for Advanced Nuclear Energy Systems*, 2004.
- [14] M. A. El-Masri. On thermodynamics of gas-turbine cycles: A model for expansion in cooled turbines. *Journal of Engineering for Gas Turbines and Power*, 1986.
- [15] W. Evans, M. Mollaghasemi, and C. Russel. Complexity of simulation models: A graph theoretic approach. *Cornell University*, 1993.
- [16] F. Fabbris. Simulazione e validazione di un modello dinamico per un impianto sperimentale a CO₂ supercritica. Master's thesis, Politecnico di Milano, 2019.
- [17] G. Ferretti. Simulation techniques and tools - [lecture notes]. *Politecnico di Milano*, 2022.
- [18] F. M. Fortuna. Analisi di configurazioni avanzate di cicli Brayton a CO₂ supercritica per generazione elettrica da cascami termici. Master's thesis, Università degli studi di Padova, 2018.
- [19] M. A. Muro Alvarado. Modelling, simulation and control of the allam cycle. Master's thesis, Politecnico di Milano, 2021.
- [20] NIST. Nist reference fluid thermodynamic and transport properties (refprop).
- [21] D. Y. Peng and D. Robinson. A new two-constant equation of state. *Industrial & Engineering Chemistry Fundamentals*, 1976.
- [22] S. Robinson. Exploring the relationship between simulation model accuracy and complexity. *Journal of the Operational Research Society*, 2022.
- [23] R. Scaccabarozzi, M. Gatti, and E. Martelli. Thermodynamic optimization and part-load analysis of the NET Power cycle. *Energy Procedia*, pages 551–560, 2017.
- [24] A. Yoonhan, J. B. Seong, and K. Minseok. Review of supercritical co2 power cycle technology and current status of research and development. *Nuclear engineering and technology*, pages 648–650, 2015.
- [25] S. A. Zaryab. Development and comparison of advanced part load control strategies for the Allam cycle. Master's thesis, Politecnico di Milano, 2018.
- [26] S. A. Zaryab, R. Scaccabarozzi, and E. Martelli. Advanced part load control strategies for Allam cycle. *Applied Thermal Engineering*, 2020.
- [27] B. Zohuri. *Gas Power and Air Cycles*. 2018.

A | Appendix A

In this appendix are reported the complete mass (A.1), momentum (A.2) and energy (A.3) balance equations that are used to model more or less every component in the cycle. These equations are then specialized and simplified by each assumption that can be done on the component, like for example its length or section or on the working fluid, for example the compressibility or the type of flow.

$$A \frac{\partial \rho}{\partial t} + \frac{\partial w}{\partial t} = 0 \quad (\text{A.1})$$

$$\frac{\partial w}{\partial t} + A \frac{\partial p}{\partial x} + \rho g A \frac{\partial p}{\partial x} + \frac{C_f}{2\rho A^2} \omega w |w| = 0 \quad (\text{A.2})$$

$$\frac{\partial h}{\partial t} + w \frac{v}{A} \frac{\partial h}{\partial x} = v \frac{\partial p}{\partial t} + v \frac{\omega}{A} \Phi_{ext} \quad (\text{A.3})$$

Where A is the cross section of the pipe, ρ is the density, w is the mass flow rate, p is the pressure, g is the gravity acceleration, z is the height of the pipe, C_f is the Fanning friction coefficient, ω is the wet perimeter, h is the fluid specific enthalpy, v is the specific volume and Φ_{ext} is the heat flux entering the pipe through the lateral surface.

In the last part of this chapter are reported the mass, momentum and energy balance equation in the case of finite volumes. As already described in 6.6.1, every heat exchanger is modeled as a continuous domain discretized in N volumes. For each volume it is possible to write the mass, momentum and energy balance equation integrating the general one-dimensional form over a constant volume, obtaining the equations in A.4, A.5 and A.6.

$$\frac{dM_i}{dy} = w_i - w_{i+1} \quad (\text{A.4})$$

$$\frac{dM_i}{dy} = -V_i \rho_{i+1}^2 \left(\frac{\partial v_{i+1}}{\partial T_{i+1}} \frac{dT_{i+1}}{dt} + \frac{\partial v_{i+1}}{\partial p_{i+1}} \frac{dp_{i+1}}{dt} \right)$$

$$p_i = p_{i+1} - kw_i \quad (\text{A.5})$$

$$\begin{aligned} \frac{dE_i}{dt} &= w_i h_i - w_{i+1} h_{i+1} + Q_i \\ \frac{dE_i}{dt} &= M_i \left(\frac{\partial u_i}{\partial T_{i+1}} \frac{dT_{i+1}}{dy} + \frac{du_{i+1}}{dp_{i+1}} + \frac{dM_i}{dt} u_i \right) \end{aligned} \tag{A.6}$$

B | Appendix B

B.1. Peng-Robinson equation of state

In order to improve the accuracy of the ideal gas law at particular conditions, for example at high pressures, during the years have been proposed a lot of possible variations. The first proposal was done by van der Waals and its cubic equation of state for fluid phase equilibrium (B.1).

$$\left(p + \frac{a}{v^2}\right)(v - b) = RT \quad (\text{B.1})$$

Where $R = \frac{R^*}{M}$ with $R^* = 8.314472$ universal gas constant, M is the molar mass, v is specific volume, T is the temperature and p is the pressure. In this new formulation appear two new parameters, a and b , which represent respectively the the attractive forces between the molecules and their size (sometimes referred to as co-volume).

Starting from this equations, a lot of improvement have been done during the years in order to take into account also the behavior of critical conditions. Among them, the most diffused are the Peng-Robinson (B.2) and Soave-Redlick-Kwong equations. The advantages related to these equations are their easiness of use and how they accurately represent the relationships among temperature, pressure, and phase compositions in binary and multicomponent systems. The performances of the two equations are very similar, except for a slightly better behaviour shown by the PREOS near the critical point. This point make the PREOS (preq) more suited to model our fluid.

$$p = \frac{RT}{(v - b)} + \frac{a(T)}{v(v + b) + b(v + b)} \quad (\text{B.2})$$

All the main parameters are described by the following equations:

$$a(T_c) = 0.45724 \frac{R^2 T_c^2}{p_c} \quad (\text{B.3})$$

$$b(T_c) = 0.07780 \frac{RT_c}{p_c} \quad (\text{B.4})$$

$$T_r = \frac{T}{T_c} \quad (\text{B.5})$$

$$\alpha(T_r, m) = (1 + m(1 - \sqrt{T_r}))^2 \quad (\text{B.6})$$

$$a(T) = a(T_c)\alpha(T_r, m) \quad (\text{B.7})$$

$$\frac{da}{dT} = -a_c m(1 + m(1 - \sqrt{T_r}))T_r^{-0.5}T_c^{-1} \quad (\text{B.8})$$

$$\frac{d^2a}{dT^2} = \frac{1}{2}a_c m(1 + m)T_r^{-\frac{3}{2}}T_c^{-2} \quad (\text{B.9})$$

B.2. Peng-Robinson equation of state for mixtures

In this section will be reported the Peng-Robinson equation in the case of mixtures [21]. This section has the scope to demonstrate how heavy could become the model increasing the complexity of the mixture. Looking at the equations here below it is straightforward to notice that the case of pure substance is much more easier to be simulated and modeled.

$$a_{ij} = (1 - \delta_{ij})\sqrt{a_i}\sqrt{a_j} \quad (\text{B.10})$$

$$a_{mix} = \sum_i^N \sum_j^N y_i y_j a_{ij} \quad (\text{B.11})$$

$$\frac{da_{mix}}{dT} = \frac{1}{2} \sum_i^N \sum_j^N y_i y_j a_{ij} \left[\frac{1}{a_i} \frac{da_i}{dT} + \frac{1}{a_j} \frac{da_j}{dT} \right] \quad (\text{B.12})$$

$$\frac{d^2a_{mix}}{dT^2} = \frac{1}{2} \sum_i^N \sum_j^N y_i y_j a_{ij} \left[\frac{1}{a_i} \frac{d^2a_i}{dT^2} + \frac{1}{a_j} \frac{d^2a_j}{dT^2} - \frac{1}{2} \left(\frac{1}{a_i} \frac{da_i}{dT} - \frac{1}{a_j} \frac{da_j}{dT} \right)^2 \right] \quad (\text{B.13})$$

$$\left. \frac{\partial h}{\partial Y_i} \right|_p = \left. \frac{\partial u}{\partial Y_i} \right|_p + p \left. \frac{\partial v}{\partial Y_i} \right|_p \quad (\text{B.14})$$

$$\left. \frac{\partial h}{\partial Y_i} \right|_p = \left. \frac{\partial h}{\partial T} \right|_p \left. \frac{\partial T}{\partial Y_i} \right|_p \quad (\text{B.15})$$

$$\left. \frac{\partial h}{\partial Y_i} \right|_p = c_p \left. \frac{\partial T}{\partial Y_i} \right|_p \quad (\text{B.16})$$

$$\left. \frac{\partial T}{\partial Y_i} \right|_p = - \left. \frac{\partial T}{\partial p} \right|_{Y_i} \left. \frac{\partial p}{\partial Y_i} \right|_T \quad (\text{B.17})$$

$$\left. \frac{\partial v}{\partial Y_i} \right|_p = - \left. \frac{\partial v}{\partial p} \right|_{Y_i} \left. \frac{\partial p}{\partial Y_i} \right|_T \quad (\text{B.18})$$

$$\left. \frac{\partial p}{\partial Y_i} \right|_{T,v} = \left[\frac{RT}{(v - b_{mix})^2} + \frac{2(v - b_{mix})}{(v(v + b_{mix}) + b_{mix}(v - b_{mix}))^2} \right] \frac{\partial b_{mix}}{\partial Y_i} + \quad (\text{B.19})$$

$$- \left[\frac{1}{v(v + b_{mix}) + b_{mix}(v - b_{mix})} \right] \frac{\partial a_{mix}}{\partial Y_i}$$

$$\frac{\partial b_{mix}}{\partial Y_i} = b_i \quad (\text{B.20})$$

$$\frac{\partial a_{mix}}{\partial Y_i} = 2 \sum_{j=1}^N Y_j a_{ij} \quad (\text{B.21})$$

$$\frac{\partial p}{\partial X_i} = \frac{\partial p}{\partial Y_i} \frac{\partial Y_i}{\partial X_i} \quad (\text{B.22})$$

B.3. Specific heat capacity at constant pressure (c_p)

$$c_v = c_p^0(T) - R + \frac{T \frac{d^2 a_{mix}}{dT^2}}{2\sqrt{2}b_{mix}} \ln \left(\frac{v + (1 + \sqrt{2})b_{mix}}{v + (1 - \sqrt{2})b_{mix}} \right) \quad (\text{B.23})$$

$$c_p = c_v - T \frac{\left(\frac{\partial p}{\partial T} \right)_v^2}{\left(\frac{\partial p}{\partial v} \right)_T} \quad (\text{B.24})$$

B.4. Enthalpy, Entropy and Internal Energy

$$h_{id} = h_0 + \int_{T_0}^T c_p^0(T) dT \quad (\text{B.25})$$

$$h_{dep} = pv - RT + \frac{T \frac{da}{dT} - a}{2\sqrt{2}b_{mix}} \ln \left(\frac{v + (1 + \sqrt{2})b_{mix}}{v + (1 - \sqrt{2})b_{mix}} \right) \quad (\text{B.26})$$

List of Figures

1.1	European energy production sources behavior [1990-2020][2]	1
1.2	Italian energy production sources in 2021[4]	2
2.1	CO ₂ phase diagram [20]	6
2.2	Density ρ	7
2.3	Specific heat C_p	7
2.4	Dynamic viscosity μ	7
2.5	Thermal conductivity k	7
2.6	Work zones for supercritical and transcritical cycles	8
2.7	Thermal efficiencies of power conversion systems with respect to the TIT	9
2.8	CO ₂ compressibility factor behavior	10
2.9	Different cycle efficiencies with respect to the TIT [13]	11
3.1	Allam cycle process flow diagram	15
3.2	Allam cycle Pressure-Specific enthalpy diagram for pure CO ₂	16
5.1	Translation stages from Modelica code to executing simulation	25
6.1	Specific enthalpy	29
6.2	Density	29
6.3	Specific heat capacity	29
6.4	Specific internal energy	29
6.5	Specific enthalpy	30
6.6	Density	30
6.7	Specific heat capacity	30
6.8	Specific internal energy	30
6.9	Specific enthalpy	31
6.10	Density	31
6.11	Specific heat capacity	31
6.12	Specific internal energy	31
6.13	Enthalpy difference at low pressure ($p = 1e5$, $T = [800-1500 \text{ }^\circ\text{C}]$)	32

6.14	Enthalpy difference at supercritical conditions ($p = 80e5$, $T = [180-620 \text{ }^\circ\text{C}]$)	33
6.15	Enthalpy difference at high pressure ($p = 300e5$, $T = [200-800 \text{ }^\circ\text{C}]$)	33
6.16	Test at low pressure conditions (C_p, ρ, u)	34
6.17	Test at slightly supercritical conditions (C_p, ρ, u)	34
6.18	Test at high pressure conditions (C_p, ρ, u)	35
6.19	Closed Allam cycle with reduced fluids	36
6.20	Compression system test model	37
6.21	Pumping system test model	38
6.22	Combustor test model	40
6.23	Turbine 2 stages	41
6.24	Turbine test model	42
6.25	Heat exchanger model block	43
6.26	Regenerator model	45
6.27	Regenerator test model	46
7.1	Open-loop fuel mass flow rate step responses	57
7.2	Open-loop pump P6 mass flow rate step responses	58
7.3	Open-loop pump Poxy mass flow rate step responses	59
7.4	Open-loop pump P5 rotational speed step responses	60
7.5	Open-loop compression system relative rotational speed step responses	61
7.6	Open-loop CPU mass flow rate step responses	62
8.1	Scheme of one intercooler in the compression system	65
8.2	Electrical equivalent circuit of the hot side of the plant	67
8.3	Net power dynamic response	72
8.4	Net power dynamic response transients	73
8.5	Turbine outlet temperature dynamic response	74
8.6	Turbine outlet temperature dynamic response transients	74
8.7	Turbine inlet temperature dynamic response	75
8.8	Turbine inlet temperature dynamic response transients	75
8.9	Pump P5 inlet pressure dynamic response	76
8.10	Pump P5 inlet pressure dynamic response transients	76
8.11	Pump P6 inlet pressure dynamic response	77
8.12	Turbine outlet pressure response	77
8.13	CPU mass flow rate dynamic response	78
8.14	CPU mass flow rate dynamic response transients	78
8.15	pumps P5-P6-Poxy mass flow rate dynamic responses	79

List of Tables

6.1	Compression system results (T - ρ)	37
6.2	Compression system results (ΔP)	37
6.3	Pumping system results	39
6.4	Combustor results	40
6.5	Turbine results at different loads	42
6.6	Regenerator results	46
6.7	Closed-cycle compression system results	48
6.8	Closed-cycle pumping system results	48
6.9	Closed-cycle combustor results	48
6.10	Closed-cycle turbine results	49
6.11	Closed-cycle regenerator results	49
8.1	Plant net power and fuel mass flow rate controlled static response	70
8.2	Turbine inlet temperature and turbine outlet pressure controlled static response	71
8.3	Regenerator outlet temperature controlled static response	71

List of Acronyms

CCS Carbon Capture and Storage

OM Open-Modelica

PREOS Peng-Robinson Equations of State

ASU Air Separation Unit

WSU Water Separation Unit

CPU CO₂ Proccession Unit

MPC Model Predictive Control

LQC Linear Quadratic Control

TIT Turbine Inlet Temperature

TOT Turbine Outlet Temperature

Acknowledgements

Like any journey, my university adventure has also come to an end. One of the fundamental things that I have learned through my years of study is that every system, to function properly, needs a reliable controller, able to constantly evaluate the state of the system, consider all possibilities, and provide the right input. The time has therefore come to thank all the "controllers" who have accompanied me over the years.

From a specialist point of view, I have to thank my supervisor, Prof. Francesco Casella, and Marcelo Andre Muro Alvarado, researcher at the Politecnico. Their help, their advices and their guidance have been essential for the realization of this project.

The biggest thanks certainly goes to my family, my mom, my dad, my sister and my grandmother, who supported me in every choice and was close to me in all situations, even when I was away. Without them I would never have been able to achieve this goal. Another big thank you goes to all my longtime friends who, despite the different paths they have taken over the years, have always been a source of great support.

I would also like to thank all the friends I've met thanks to the university, with whom I've shared most of these five years and countless train journeys, between study afternoons and card games.

Finally, I would like to thank all my students at the high school Badoni of Lecco, who have accompanied me in these last months of thesis drafting. Thanks to their cheerfulness, light-heartedness and sometimes very little desire to follow the lessons, they helped me take a break from the long days at the PC.

Thank you all.

Ringraziamenti

Come qualsiasi viaggio, anche il mio percorso universitario è giunto al termine. Una delle cose fondamentali che ho appreso grazie ai miei anni di studi è che ogni sistema, per funzionare correttamente, ha bisogno di un controllore affidabile, in grado di valutare costantemente l'insieme degli eventi, prendere in considerazione tutte le possibilità, e fornire il giusto input. È quindi giunto il momento di ringraziare tutti i "controllori" che mi hanno accompagnato in questi anni.

Dal punto di vista specialistico non posso che ringraziare il mio relatore, il Prof. Francesco Casella, e Marcelo Andre Muro Alvarado, ricercatore presso il Politecnico. Il loro aiuto, i loro consigli e la loro guida sono stati fondamentali per la realizzazione di questo progetto.

Il più grande ringraziamento va sicuramente alla mia famiglia, mia mamma, mio papà, mia sorella e mia nonna, che mi ha supportato in ogni scelta e mi è stata vicina in tutte le situazioni, anche quando io ero lontano. Senza di loro non sarei mai riuscito a raggiungere questo obiettivo.

Un altro grande ringraziamento va a tutti i miei amici di lunga data che, nonostante le strade diverse intraprese negli anni, sono sempre stati fonte di grande supporto.

Vorrei anche ringraziare tutti gli amici che ho conosciuto grazie all'università, con i quali ho condiviso gran parte di questi cinque anni ed innumerevoli viaggi in treno, tra pomeriggi di studio e partite di carte.

Infine vorrei ringraziare tutti i miei studenti dell'istituto superiore Badoni di Lecco, che mi hanno accompagnato in questi ultimi mesi di stesura della tesi. Grazie alla loro allegria, spensieratezza e a volte pochissima voglia di seguire le lezioni, mi hanno aiutato a prendermi una pausa dalle lunghe giornate al pc.

Grazie a tutti.

